State of the Global Climate 2023

WEATHER CLIMATE WATER

WORLD METEOROLOGICAL ORGANIZATION

WMO-No. 1347

SUBJECT TO COPY EDIT

Cover illustration: A melting glacier with chunks of ice breaking apart. The background captures the consequences of global warming on ice formations. Generative AI. Par Regina. N° de fichier: 640624130

Contents

We need your feedback

This year, the WMO team has launched a process to gather feedback on the State of the Climate reports and areas for improvement. Once you have finished reading the publication, we ask that you kindly give us your feedback by responding to this short survey. Your input is highly appreciated.

Key messages

2023 was the warmest year on record at 1.45 ± 0.12 °C above the pre-industrial average.

Concentrations of the three main greenhouse gases – carbon dioxide, methane, and nitrous oxide – reached record high observed levels.

Ocean heat content reached its highest level in the 65-year observational record.

Global mean sea level reached a record high. The rate of sea level rise in the past ten years (2014–2023) has more than doubled since the first decade of the satellite record (1993–2002).

Antarctic sea-ice extent reached an absolute record low in February. The annual maximum extent was around 1 million km^2 below the previous record low maximum.

Preliminary data from the global set of reference glaciers for the hydrological year 2022-2023 show they experienced the largest loss of ice on record (1950–2023), driven by extremely negative mass balance in both western North America and Europe.

Glaciers in Switzerland lost around 10% of their remaining volume in the past two years.

Extreme weather continued to lead to severe socio-economic impacts. Extreme heat affected many parts of the world. Wildfires in Hawaii, Canada and Europe led to loss of life, the destruction of homes and large-scale air pollution. Flooding associated with extreme rainfall from Mediterranean Cyclone Daniel affected Greece, Bulgaria, Türkiye, and Libya with particularly heavy loss of life in Libya.

Food security, population displacement and impacts on vulnerable populations continue to be of mounting concern in 2023, with weather and climate hazards exacerbating the situation in many parts of the world.

Foreword

The World Meteorological Organization State of the Global Climate report confirms that the year 2023 broke every single climate indicator.

It was by far the warmest year on record. The global average temperature in 2023 was 1.45 ± 0.12 °C above the 1850–1900 average. Never have we been so close – albeit on a temporary basis – to the 1.5° C lower limit of the Paris Agreement on climate change.

Concentrations of greenhouse gases continued to rise. Ocean heat content and sea level reached record observed highs, and the rate of increase is accelerating. Antarctic sea ice extent hit record observed lows. Key glaciers suffered record losses.

The climate crisis is the defining challenge that humanity faces.

Heatwaves, floods, droughts, wildfires and intense tropical cyclones wreaked havoc on every continent and caused huge socio-economic losses. There were particularly devastating consequences for vulnerable populations who suffer disproportionate impacts.

Extreme climate conditions exacerbated humanitarian crises, with millions experiencing acute food insecurity and hundreds of thousands displaced from their homes.

WMO is committed to stepping up collaboration with the international community to confront the enormity of this challenge.

WMO and its Members are expanding life-saving early warning services to achieve the ground-breaking Early Warnings For All initiative. A new Global Greenhouse Gas Watch seeks to provide scientifically-based information for climate change mitigation. The transition to renewable energy must be supported by tailor-made weather and climate services.

To succeed, it is imperative to leverage efforts across the entire value chain—from improving climate data and monitoring, strengthening prediction and projections, and building capacity. We must make climate information more accessible and actionable to serve society.

I hope this report will raise awareness of the vital need to scale up the urgency and ambition of climate action.

I take this opportunity to congratulate and thank the experts and lead authors who compiled this report. I extend my gratitude to all the contributors, National Meteorological and Hydrological Services and Regional Climate Centres and United Nations agencies.

(Prof. Celeste Saulo)
Secretary-General

Global climate indicators

The global climate indicators provide an overview of changes in the climate system.[1] The set of interlinked physical indicators presented here connect the changing composition of the atmosphere with changes in energy in the climate system and the response of land, ocean, and ice.

The global indicators are based on a wide range of data sets which comprise data from multiple observing systems including satellites and in situ networks (for details on data sets used in the report, see Data set and methods).

Changes to the physical climate, measured here by key indicators, can have cascading impacts on national development and progress toward the UN Sustainable Development Goals (SDGs).[2] For example, changes in the acidity or temperature of the ocean can affect marine life, potentially impacting coastal communities that may depend on the local catch for their livelihood or food security. On the other hand, climate science has a critical role to play in facilitating sustainable development. As demonstrated by the 2023 United in Science report, weather, climate, and water-related sciences support the achievement of many of the SDGs.[3] Recognizing the interconnections between climate and development can therefore lead to synergistic action—an increasing necessity as the world gets further off-track from achieving both the SDGs and the Paris Agreement goals.[4]

BASELINES

Baselines are periods of time, usually spanning three decades or more, that are used as a fixed benchmark against which current conditions can be compared. For scientific, policy and practical reasons, several different baselines are used in this report, and these are specified in the text and figures. Where possible, the most recent WMO climatological standard normal, 1991–2020, is used for consistent reporting.

For some indicators, however, it is not possible to use the standard normal owing to a lack of measurements during the early part of the period. There are also two specific exceptions. First, for the global mean temperature time series – and only for the global mean series – a reference period of 1850–1900 is used. This is the baseline used in IPCC AR6 WG I as a reference period for pre-industrial conditions and is relevant for understanding progress in the context of the Paris Agreement. Second, greenhouse gas concentrations can be estimated much further back in time using gas bubbles trapped in ice cores. Therefore, the year 1750 is used in this report to represent pre-industrial greenhouse gas concentrations.

GREENHOUSE GASES

Concentrations of the three main greenhouse gases – carbon dioxide, methane, and nitrous oxide – reached record high observed levels in 2022, the latest year for which consolidated global values are available (1984–2022). Real-time data from specific locations show that levels of the three greenhouse gases continued to increase in 2023.

Atmospheric concentrations of greenhouse gases reflect a balance between emissions from human activities, natural sources, and sinks. Increasing levels of greenhouse gases in the atmosphere due to human activities have been the major driver of climate change since the industrial revolution. Global average mole fractions of greenhouse gases – referred to here for simplicity as the "concentration" in the atmosphere – are calculated from in situ observations made at multiple sites through the Global Atmosphere Watch (GAW) Programme of WMO and partner networks.

In 2022 – the latest year for which consolidated global figures are available – atmospheric levels of greenhouse gases reached new observed highs (Figure 1), with globally averaged concentrations for carbon dioxide (CO_2) at 417.9 ± 0.2 parts per million (ppm), methane (CH_4) at 1923 ± 2 parts per billion (ppb) and nitrous oxide (N_2O) at 335.8 ± 0.1 ppb, respectively 150%, 264% and 124% of pre-industrial (1750) levels. The rate of increase of CH_4 was the second highest on record, after 2021, and the rate of increase of N_2O was the highest on record. The rate of increase of CO_2 at 2.2 ppm was slightly below the 10-year average of 2.46 ppm·yr^{-1}. CO_2 growth rate is typically lower in years which start with La Niña, as 2022 did, and higher in years which start with El Niño as 2016 did.[5] Real-time data from specific locations, including Mauna Loa[6] (Hawaii, United States of America) and Kennaook/Cape Grim[7] (Tasmania, Australia) indicate that levels of CO_2, CH_4 and N_2O continued to increase in 2023.
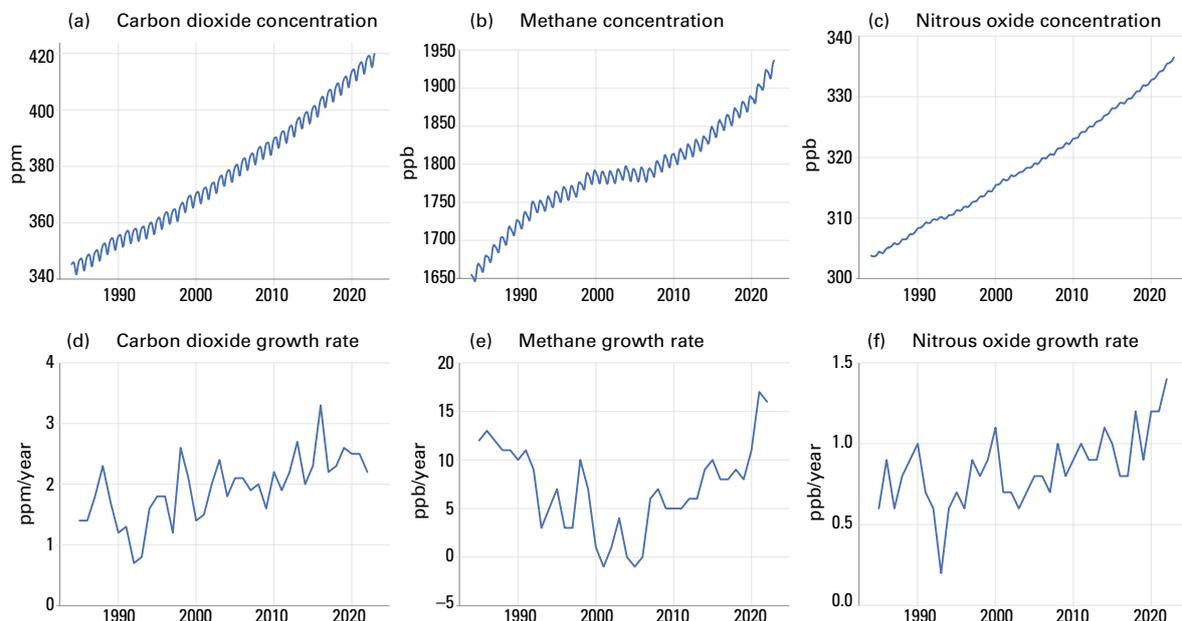
Figure 1. Top row: Monthly globally averaged mole fraction (measure of atmospheric concentration), from 1984 to 2022, of (a) CO_2 in parts per million, (b) CH_4 in parts per billion and (c) N_2O in parts per billion. Bottom row: the growth rates representing increases in successive annual means of mole fractions for (d) CO_2 in parts per million per year, (e) CH_4 in parts per billion per year and (f) N_2O in parts per billion per year.

TEMPERATURE

The global mean near-surface temperature in 2023 was 1.45 ± 0.12 °C above the 1850–1900 average. 2023 was the warmest year in the 174-year observational record, clearly surpassing the previous joint warmest years, 2016 at 1.29 ± 0.12 °C above the 1850–1900 average and 2020 at 1.27±0.13 °C.

The past nine years, 2015–2023, were the nine warmest years on record.

Record monthly global near-surface temperatures have been observed for the ocean – from April through to December – and, starting slightly later, the land – from July through to November.

The ten-year average 2014–2023 global temperature is 1.20±0.12°C above the 1850–1900 average, the warmest 10-year period on record.

Global mean near-surface temperature in 2023 was 1.45 ± 0.12 °C above the 1850–1900 average[8] (Figure 2). The analysis is based on a synthesis of six global temperature datasets (see Data set and methods). 2023 was the warmest year in the 174-year instrumental record in each of the six data sets. The past nine years – 2015 to 2023 – were the nine warmest years on record. The two previous warmest years were 2016 with an anomaly of 1.29 ± 0.12 °C, and 2020 with an anomaly of 1.27 ± 0.13 °C.

The second-highest margin by which a September record was broken in the past 60 years (the period covered by all datasets) was substantially smaller, at 0.03 to 0.17 °C in 1983. July is typically the warmest month of the year globally, and thus July 2023 became the warmest month on record.

The long-term increase in global temperature is due to increased concentrations of greenhouse gases in the atmosphere. The shift from La Niña, which lasted from mid-2020 to early 2023, to fully developed El Niño conditions by September 2023 (see Short-term climate drivers) likely explains some of the rise in temperature from 2022 to 2023. However, some areas of unusual warming such as the Northeast Atlantic (Figure 3) do not correspond to typical patterns of


Created 2024-02-18 15:42:33
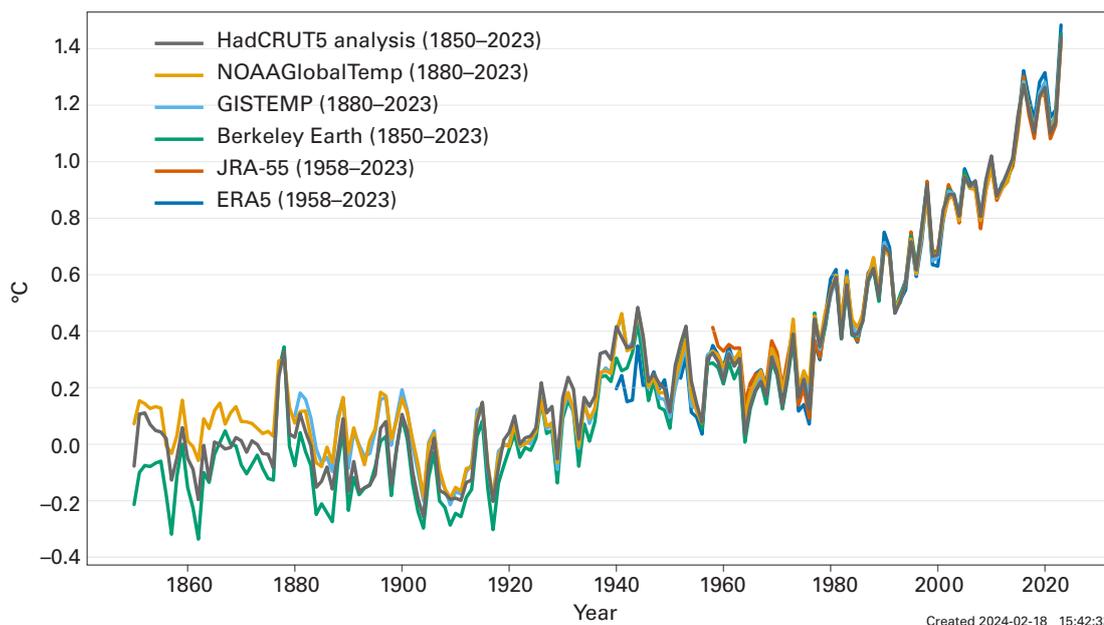
Figure 2. Annual global mean temperature anomalies (relative to 1850–1900) from 1850 to 2023. Data are from six data sets as indicated in the legend, see Data set and methods for details.

Created: 2024-02-14 11:29:40
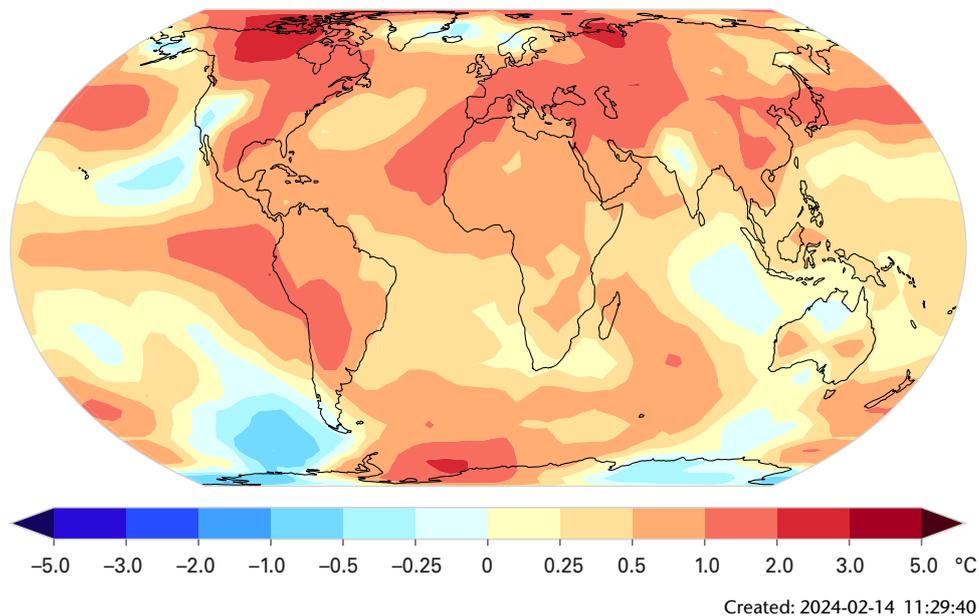
Figure 3. Mean near-surface temperature anomalies (difference from the 1991–2020 average) for 2023. Data are the median of six data sets as indicated in the legend, see Data set and methods for details.

warming or cooling associated with El Niño. Other factors, which are still being investigated, may also have contributed to the exceptional warming from 2022 to 2023 and it is unlikely to be due to internal variability alone.[9]

The average global temperature over the past ten years, 2014 to 2023, was 1.20 ± 0.12 °C above the 1850–1900 average, making the past ten years the warmest among all ten-year periods on record in all six datasets.

Between late Northern Hemisphere spring and the end of the year, global average sea-surface temperatures (SSTs) were also at a record observed high The records for July, August and September were each broken by a large margin (around 0.21 to 0.27 °C). Exceptional warmth relative to the 1991–2020 baseline, was recorded in the eastern North Atlantic, the Gulf of Mexico and the Caribbean, the North Pacific extending eastward from the Sea of Japan, the Arabian Sea, and large areas of the Southern Ocean (Figure 3, see also Marine heatwaves and cold spells).

Observed global land temperature anomalies reached record levels in July and August, somewhat later than for the SSTs, but the September average was also a record by a large margin of 0.53 to 0.71 °C. The second-widest margin by which a record has been broken in the past 60 years was 0.22 to 0.27 °C in September 2002. In 2023, most land areas were warmer than the 1991–2020 average (Figure 3). Unusual warmth was reported across large areas of northern Canada, the southern U.S., Mexico, and Central America, as well as large areas of South America. Large areas from central Asia to western Europe including parts of North Africa and the Arabian Peninsula were also unusually warm, as were southeast Asia, and Japan.

OCEAN

Increasing human emissions of CO_2 and other greenhouse gases cause a positive radiative imbalance at the top of the atmosphere, meaning energy is being trapped within the climate system. The imbalance leads to an accumulation of energy in the Earth system in the form of heat that is driving global warming.[10,11] The ocean, which covers around 70% of the Earth's surface, absorbs heat and CO_2, which can act to slow the rate of warming in the atmosphere. However, the heat absorbed by the ocean leads to ocean warming which, together with the melting of ice on land, raises sea levels. The ocean also absorbs CO_2 leading to ocean acidification. Warming waters, sea level rise and ocean acidification all have significant effects on the ocean, as well as the plants and animals that live in it and the people who rely upon it for their livelihoods.

OCEAN HEAT CONTENT

In 2023, ocean heat content reached its highest level in the 65-year observational record.

Around 90% of the energy that has accumulated in the Earth system since 1971 is stored in the ocean. As energy has accumulated in the ocean, it has warmed and the heat content of the ocean (Ocean Heat Content, Figure 4) has increased.

According to a consolidated analysis based on several individual datasets, the upper 2000 m of the ocean continued to warm in 2023.[12] It is expected that warming will continue – a change which is irreversible on centennial to millennial timescales.[13,14] Ocean heat content in 2023 was the highest on record, exceeding the 2022 value by 13 ± 9 ZJ (Figure 4) consistent with estimates published early in 2024.[15]

All data sets agree that ocean warming rates show a particularly strong increase in the past two decades. The rate of ocean warming for the 0–2000 m layer was 0.7 ± 0.1 W·m^{-2} from 1971–2023 on average, but 1.0 ± 0.1 W·m^{-2} from 2005-2023 (the period covered by the Argo programme). The steady increase of ocean warming rates[16,17] is seen consistently in direct estimates from in situ observations, indirect estimates from remote sensing, and direct estimate of the net flux at the top of the atmosphere as measured by satellites.[18] Different drivers of this change are discussed in literature, including a change in anthropogenic climate forcing[19] and natural variability.[20] Deep-ocean global warming below 2000 m depth is estimated to be 0.07 ± 0.03 W·m^{-2} from 1992–2022.[21]
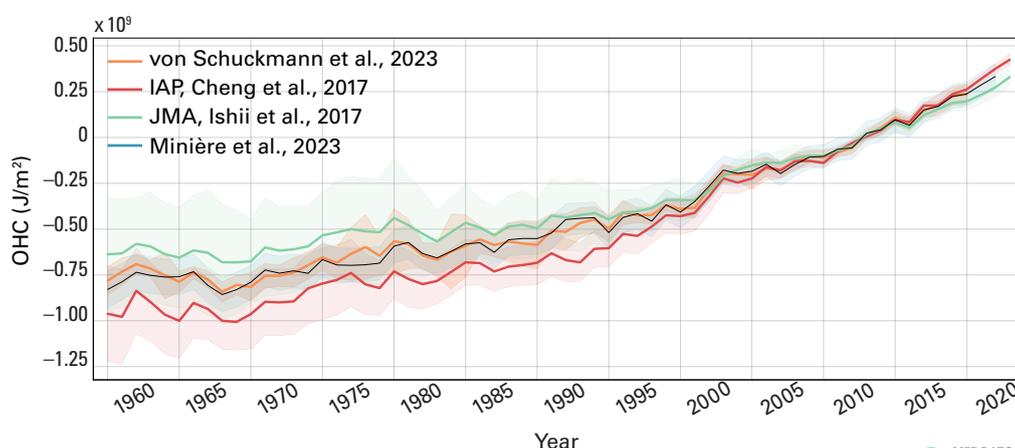
**Figure 4.** Global ocean heat content (OHC) anomalies relative to the 2005–2021 average for the 0–2000 m depth layer 1960–2023. Ensemble mean time series and ensemble standard deviation (2-standard deviations, shaded) updated from von Schuckmann et al. (2023) (orange). Updated from Cheng et al. (red) 2017. From Minière et al. 2023 (blue). Updated from Ishii et al. 2017 (green).

Source: Mercator Ocean international.

Although ocean heat content (OHC) has increased strongly through the entire water column, the rate of warming has not been the same everywhere.[22] The strongest warming in the upper 2000 m occurred in the Southern Ocean (60°S-35°S), North Atlantic (20°N–50°N) and South Atlantic (60°S–0°S) (Figure 5). The Southern Ocean domain is the largest reservoir of heat, accounting for[23] around 32% of the global OHC increase in the upper 2000 m since 1958. The Atlantic Ocean accounts for approximately 31% of the global 0–2000 m OHC increase; the Pacific Ocean around 26%.

Some relatively small regions are cooling, including the subpolar North Atlantic Ocean extending from near the surface down to a depth of over 800 m (also the only area to show centennial cooling at the surface). The contrasting pattern of cooling (50°N–70° N) and warming (20°N–50°N) in the North Atlantic has been associated with a slowing of the Atlantic Meridional Overturning Circulation and local interactions between the air and sea.[24] Other cooling regions include the northwest Pacific, southwest Pacific and southwest Indian Oceans.

SEA LEVEL

In 2023, global mean sea level reached a record high in the satellite record (1993 to present), reflecting continued ocean warming as well as the melting of glaciers and ice sheets.

The rate of global mean sea level rise in the past ten years (2014–2023) is more than twice the rate of sea level rise in the first decade of the satellite record (1993–2002).

Global mean sea level (GMSL) continued to rise in 2023 (Figure 6). The La Niña conditions between mid-2020 and early 2023 had only a small apparent effect on GMSL, unlike the 2011 La Niña that led to a temporary decrease in the GMSL of several millimetres. The rapid rise observed in 2023 is likely due in part to El Niño. The long-term rate of sea level rise has more than doubled since the start of the satellite record, increasing from 2.13 mm·yr^{-1} between 1993 and 2002 to 4.77 mm·yr^{-1} between 2014 and 2023.
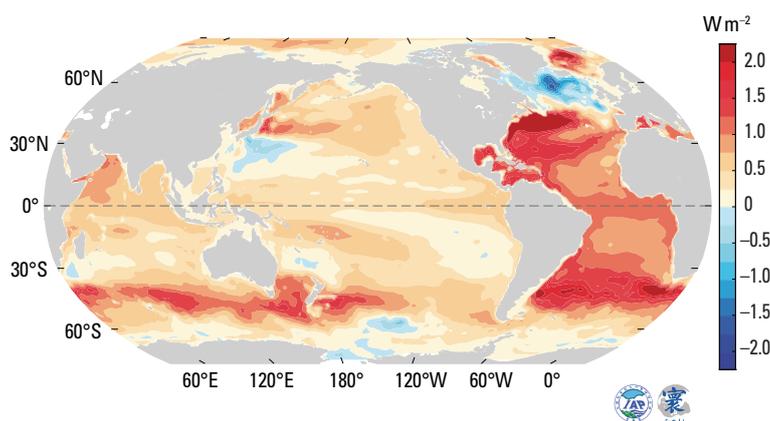
Figure 5. Observed upper 2000 m OHC trend from 1958 to 2023.

Source: Data updated from Cheng et al.[25]
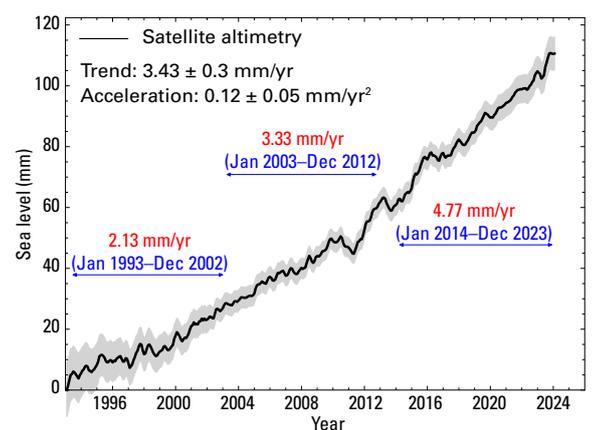
Figure 6. GMSL evolution between January 1993 and December 2023 based on satellite altimetry. The black line is the best estimate, and the grey shaded area indicates the uncertainty. Red and blue annotations indicate the average rate of sea level rise during three decades of the record as indicated.

Source: AVISO altimetry (https://www.aviso.altimetry.fr).
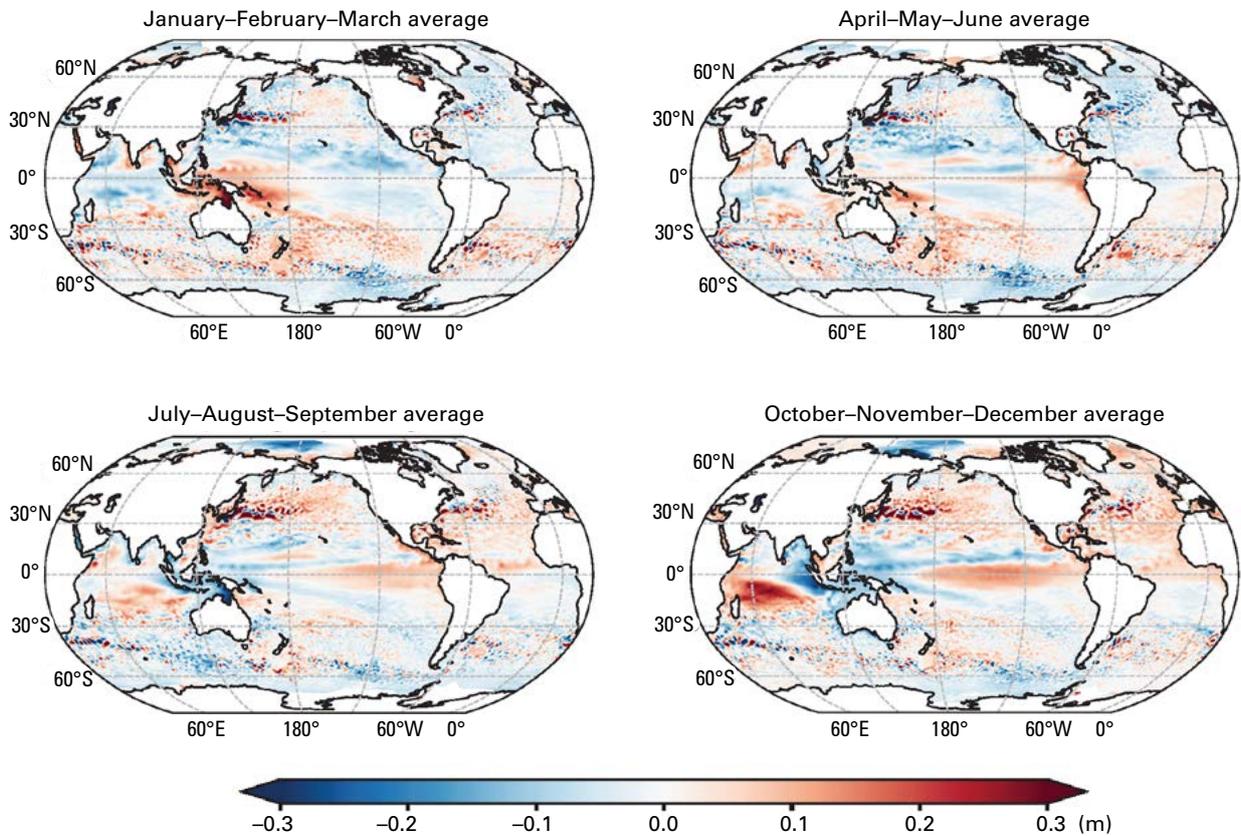
Figure 7. 3-month averages of altimetry-based sea level anomalies (relative to the 1993–2012 average, which is the product climatology) for January to March 2023 (top left), April to June 2023 (top right), July to September 2023 (bottom left) and October to December 2023 (bottom right).

Source: Data downloaded from the Copernicus Marine Service (CMEMS, https://marine.copernicus.eu).

From January to March 2023, sea levels (Figure 7) were higher than the long-term average (1993–2012) in the western tropical Pacific. This is characteristic of warm seawater in the region associated with ENSO-neutral conditions. Sea levels in the North Atlantic and eastern tropical Pacific were lower than the long-term average. Warming of the surface waters in the eastern tropical Pacific during the early stages of the 2023 El Niño (see Short-term climate drivers) led to an increase in sea level relative to the long-term mean in the most eastern part of the tropical Pacific between April and June. By July to September, the El Niño signature was clearly visible, with sea level being above average from the mid-tropical Pacific to the coasts of central and South America. Above average sea levels were also observed in the tropical and north-east Atlantic, associated with the anomalous warming in these areas during Northern Hemisphere summer. From October to the end of the year, the El Niño pattern continued to develop. The shift to the positive phase of the Indian Ocean Dipole also led to higher-than-average sea level in the western Indian Ocean and lower-than-average sea levels in the east (see Short-term climate drivers).

MARINE HEATWAVES AND COLD SPELLS

As with heatwaves and cold-spells on land, marine heatwaves (MHW) and marine cold-spells (MCS) are prolonged periods of extreme high or low temperatures in the seas and ocean that can have a range of consequences for marine life and dependent communities.[26] MHWs have become more frequent, intense, and longer lasting since the late 20th century, while MCSs have been decreasing by those same measures. Satellite retrievals of sea-surface temperature are used to monitor MHWs and MCSs globally, categorized here as *moderate*, *strong*, *severe*, extreme, or ice (for definitions, see Data set and methods).

El Niño events tend to cause wide-spread MHWs in the eastern Tropical Pacific. While this region did experience *strong* MHWs in 2023 to late October (Figure 8a), and *moderate* for the rest of 2023, the overall areal coverage was smaller in area than it was in previous El Niño events.

(a)
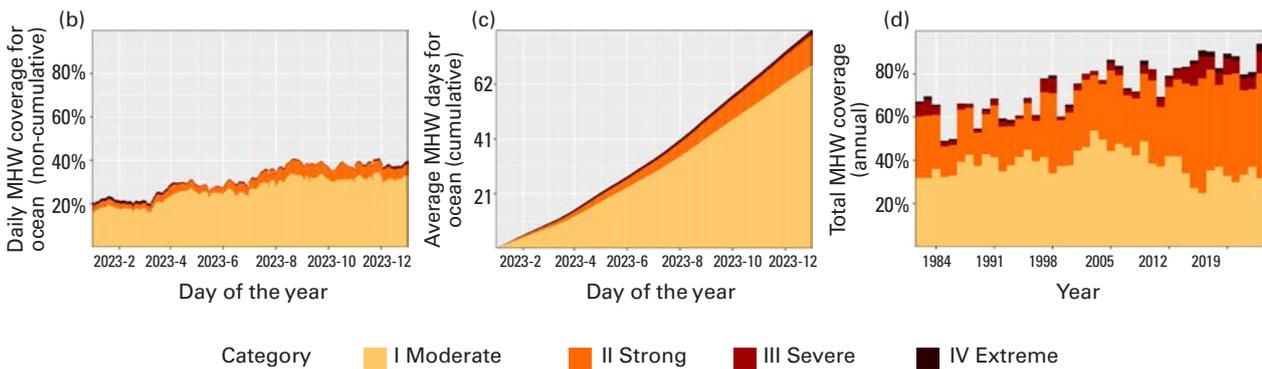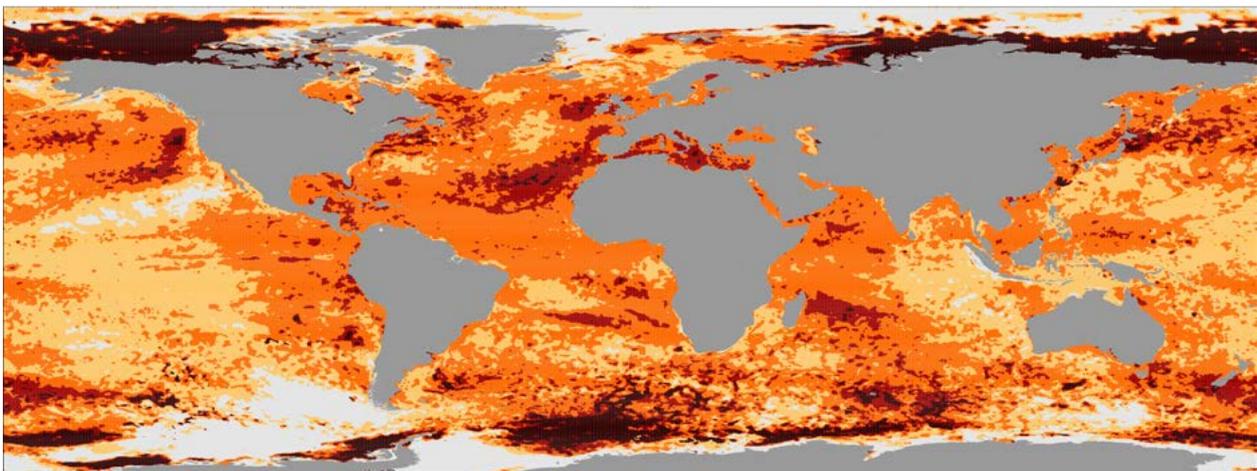
Figure 8. (a) Global map showing the highest MHW category (for definitions, see Data set and methods) experienced at each pixel over 2023 (reference period 1982–2011). Light grey indicates that no MHW occurred in a pixel over the entire year; (b) Stacked bar plot showing the percentage of the surface of the ocean experiencing an MHW on any given day of the year; (c) Stacked bar plot showing the cumulative number of MHW days averaged over the surface of the ocean. Note: This average is calculated by dividing the cumulative sum of MHW days per pixel weighted by the surface area of those pixels. (d) Stacked bar plot showing the total percentage of the surface of the ocean that experienced a MHW from 1982 to present. Data are from National Oceanic and Atmospheric Administration (NOAA) Optimum Interpolation Sea-Surface Temperature (OISST).

Source: Robert Schlegel

Of note in 2023 were the persistent and wide-spread MHWs in the North Atlantic which began in the Northern Hemisphere spring, peaked in extent in September and persisted through to the end of the year. While the area of the event diminished into December, the intensity increased. The end of 2023 saw a broad band of *severe* and *extreme* MHWs across the North Atlantic, with temperature anomalies in the open ocean of +3 °C.

The Mediterranean Sea was also unusually warm relative to the baseline period and experienced near complete coverage of *strong* and *severe* MHWs for the twelfth consecutive year. In the southern hemisphere, the waters surrounding New Zealand remained 1 to 2 °C above the long-term average through January to September (~270 days).

At the end of 2023, most of the global ocean from roughly 20° North to South of the equator had been in a MHW state since early November. In contrast, there were almost no occurrences of MCSs within 60° North or South of the equator in 2023 (Figure 9a).

The global ocean experienced an average daily MHW coverage of 32% (Figure 8b), well above the previous record of 23% in 2016. In contrast, the average daily coverage of MCS (Figure 9b) was only 4%, far below 2022 (7%).
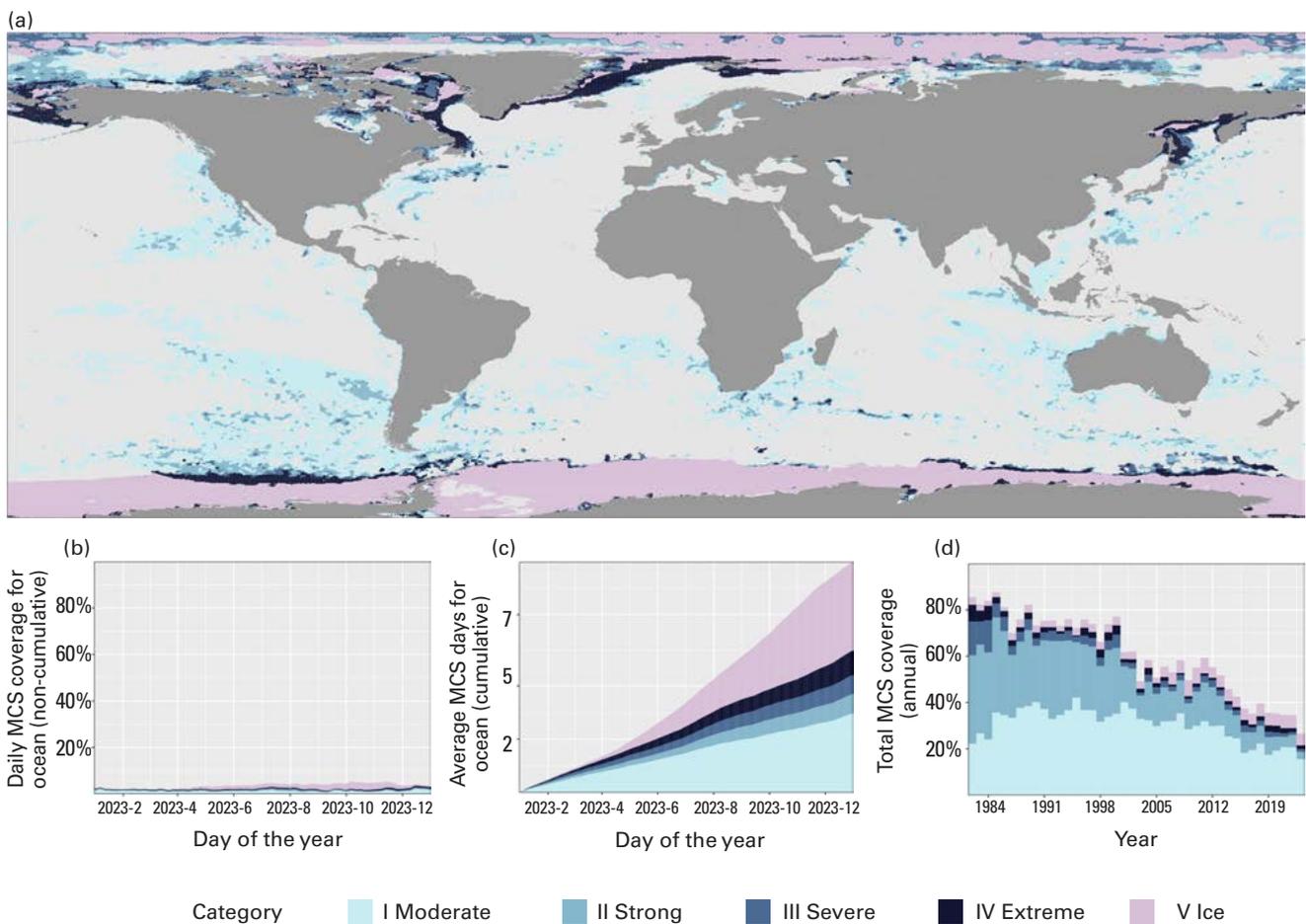

Figure 9. As for Figure 8 but showing marine cold-spells rather than marine heatwaves. Data are from NOAA OISST.

Source: Robert Schlegel.

OCEAN ACIDIFICATION

The ocean absorbs around one quarter of the annual emissions of anthropogenic CO_2 to the atmosphere.[27,28] CO_2 reacts with seawater and alters the carbonate chemistry, resulting in a decrease in pH referred to as "ocean acidification" (Figure 10). Ocean acidification affects organisms and ecosystem services, including food security, by reducing biodiversity, degrading habitats, and endangering fisheries and aquaculture.[29] The IPCC AR6 concluded that "There is very high confidence that open ocean surface pH is now the lowest it has been for at least 26 [thousand years] and current rates of pH change are unprecedented since at least that time".[30]

Although global efforts, many supported by IOC-UNESCO and led by the Global Ocean Acidification Observing Network and its UN Ocean Decade Programme – Ocean Acidification Research for Sustainability, have resulted in an increase in the number of ocean acidification observations, many regions remain under-sampled. Data collected for the Sustainable Development Goal 14.3.1 Indicator ("Average marine acidity (pH) measured at agreed suite of representative sampling stations") show that the current coverage is inadequate (Figure 11), with time series not long enough to determine trends and gaps in observations in all areas. Global trends illustrating the decrease of the global pH (Figure 10) show the large-scale effects of CO_2 emissions. However, the rate of change in ocean acidification, and its pattern and scale, show great regional and temporal variability and understanding these requires high-resolution, long-term observation at scales relevant to the affected communities.
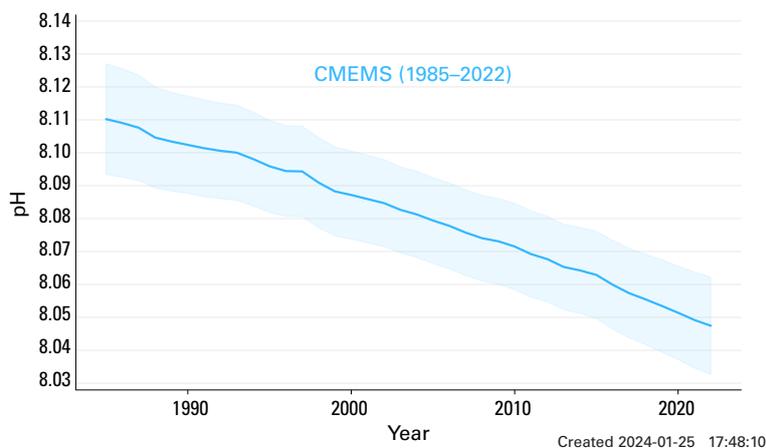
Figure 10. Global annual mean ocean surface pH (purple) covering the period 1985–2022. The shaded area indicates the estimated uncertainty in the values.

Source: Data from Copernicus Marine Environment Monitoring Service.
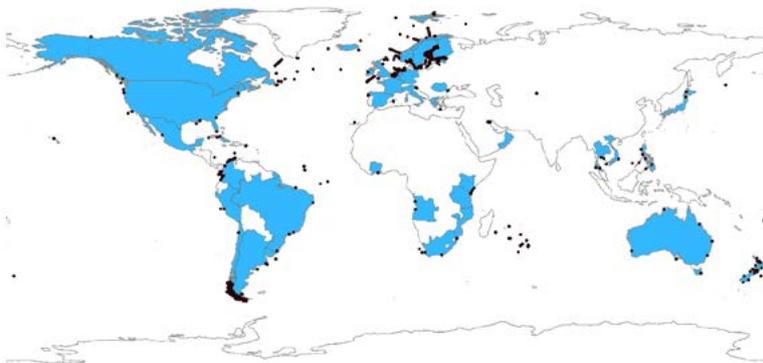
Figure 11. Map illustrating surface ocean carbonate chemistry measurement locations received for SDG indicator 14.3.1 ocean acidification reporting by IOC/UNESCO. Countries highlighted in light blue colour reported data in accordance with the SDG 14.3.1 Indicator Methodology. Black dots show the location of sampling stations from which data was collected.

CRYOSPHERE

The cryosphere comprises the frozen parts of Earth – glaciers and ice sheets, sea-ice, snow, and permafrost. The inhospitable and often remote environments in which ice forms mean that it has sometimes been challenging to undertake long-term measurements of the cryosphere. At the same time, the profound changes seen in the cryosphere clearly illustrate the global scale of climate change.

SEA-ICE

Arctic sea-ice extent remained well below normal in 2023, with the annual maximum and annual minimum extents being respectively the fifth and sixth lowest in the 45-year satellite record.

Antarctic sea-ice extent reached an absolute record low for the satellite era (1979 to present) in February. Ice extent was at a record low for the time of year from June till early November, and the annual maximum in September was around 1 million km^2 below the previous record low maximum.

Arctic sea-ice extent reached its annual maximum of 14.62 million km^2 on 6 March, the fifth lowest in the satellite record.[31] The annual minimum Arctic sea-ice extent was reached on 19 September[32] (Figure 12), with a minimum extent of 4.23 million km^2, well below the long-term average (1991–2020) of ~5.5 million km^2. This was the sixth lowest minimum Arctic sea-ice extent in the satellite record (1979–2023), not as extreme as 2012 or 2020 but only slightly higher than 2007, 2016 and 2019, and continuing the long-term trend of reduced late-summer and early-autumn Arctic ice cover. Major negative anomalies were observed in the Beaufort, Chukchi, and East Siberian Seas (Figure 12 right). The year ended with extents close to the long-term average, but still the 9th lowest in the satellite record.[33]
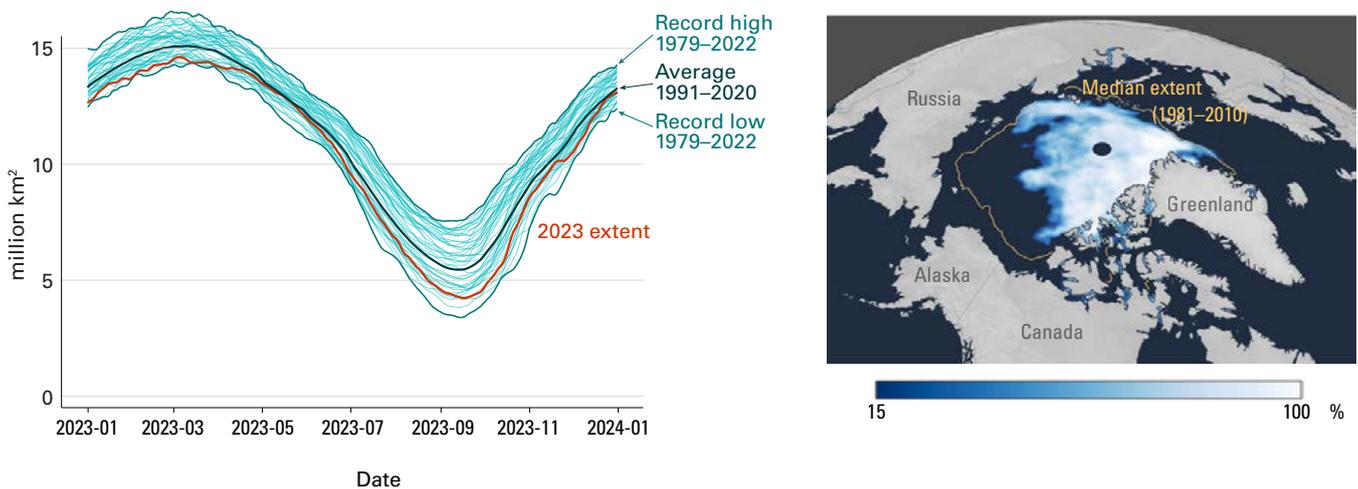
Figure 12. (left) Daily Arctic sea-ice extent from January through December, showing 2023 (red line) against the climate normal (1991–2020, dark blue) and the record highest and lowest extents for each day (mid blue). Individual years are shown in light blue. (right) Ice concentration on September 19, 2023, at the annual minimum Arctic ice extent. The yellow line indicates the median ice edge for the 1981–2010 period.[34]

*Source:* Data and map from the U.S. National Snow and Ice Data Center.
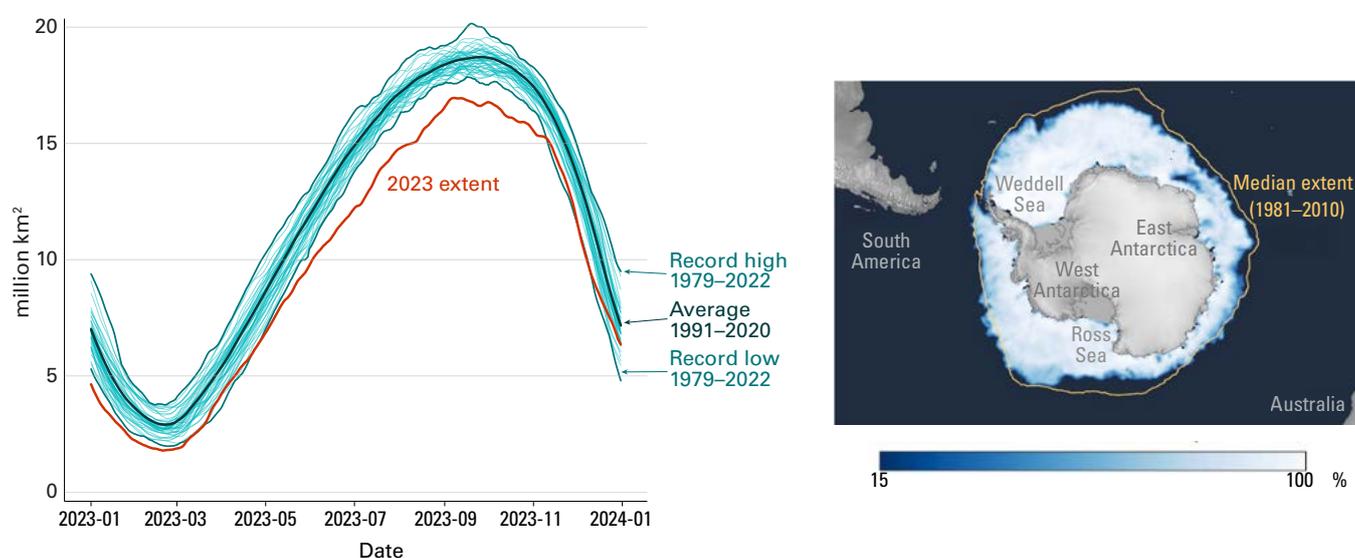
Figure 13. (left) Daily Antarctic sea-ice extent from January through December, showing 2023 (red) conditions against the 1991–2020 climate normal (dark blue) and the record highest and lowest extents for each day (mid blue). Individual years are shown in light blue. (right) Ice concentration on September 10, 2023, the 2023 annual maximum extent. The yellow line shows the median ice edge for the 1981–2010 climatology period.[39]

Source: Data and map from the U.S. National Snow and Ice Data Center.

Antarctic sea-ice extent declined to 1.79 million km^2 on February 21, 2023 (Figure 13), an all-time minimum for the satellite era (1979 to present), slightly less than the previous record low that was set in 2022.[35] Sea-ice extent remained below the average as the growth season commenced, becoming record low for the time of year in May. Slow growth continued with exceptional record low extents between July and the annual maximum, likely in association with warming of the Southern Ocean.[36] The maximum Antarctic sea-ice extent for 2023 (Figure 13) was 16.96 million km^2 on 10 September, roughly 1.5 million km^2 below the 1991–2020 average and 1 million km^2 below the previous record low maximum set in 1986.[37] Record low extents for the time of year continued until early November but a slower-than-average rate of decline in December brought ice extents closer to the long-term mean by the end of the year.[38]

ICE SHEETS

> It was the warmest summer on record at the Summit station, 3.4 °C warmer than the 1991–2020 average and 1.0 °C warmer than the previous record.

An ice sheet is an expanse of ice originating on land that covers an area of more than 50 000 km^2.[40] There are two principal ice sheets in the present-day climate system, in Greenland and Antarctica. The total mass balance (TMB) of an ice sheet is the sum of three components: the surface mass balance (SMB), the marine mass balance (MMB), and the basal mass balance (BMB). The SMB is the difference between snow accumulation and meltwater runoff from the ice sheet. The MMB is the mass loss at the edge of the ice sheet from the calving of icebergs and the melting of ice that is in contact with the ocean. BMB consists of melting at the ice sheet bed due to geothermal heat and friction as the ice slides over the ground beneath. A negative mass balance indicates a loss of ice mass; a positive mass balance indicates a gain.
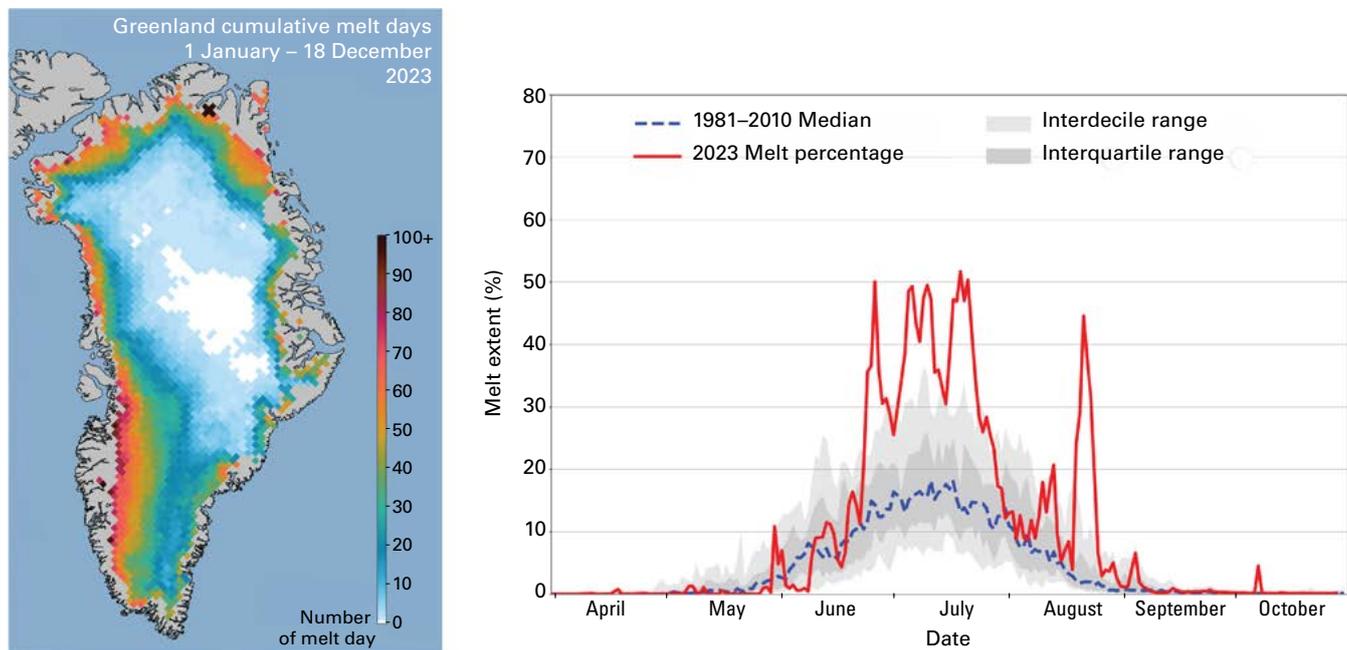
Figure 14. Greenland Ice Sheet melt conditions through 2023: (left) Cumulative melt days for Greenland in 2023. White areas indicate no melting occurred. (right) Percentage of the ice sheet experiencing melting conditions each day.

Source: Images and analysis courtesy of Thomas Mote, University of Georgia, and the U.S. National Snow and Ice Data Center..

The Greenland Ice Sheet continued to lose mass in the hydrological year 2022–2023 (1 September 2022 to 31 August 2023) based on estimates from an ensemble of regional climate models.[41] Annual snow accumulation over Greenland still exceeds surface melt in most years, giving a positive SMB. For 2022–2023 this was estimated at +317 Gt, below the long-term average but well above the extreme melt years of 2011–2012 and 2018–2019. Combined with BMB (–27 Gt) and MMB (–504 Gt), the estimated 2022–2023 ice sheet total mass balance was about –217 Gt.

The summer 2023 melt season was relatively intense, punctuated by major heat waves in July and August.[42] Satellite melt-extent data indicate that the ice sheet had the third highest cumulative melt-day area[43] on record (1978–2023), after the extreme melt season of 2012 and 2010 (Figure 14). It was the warmest summer on record (1987-present) at the Summit station, 3.4 °C warmer than the 1991–2020 average and 1.0 °C warmer than the previous record.[44] Summit station experienced melting conditions for the fifth year on record (2012, 2019, 2021, 2022, 2023); ice core records indicate that significant, melting conditions last happened in the late nineteenth century.[45]

The Ice Sheet Mass Balance Intercomparison Exercise (IMBIE) has documented the acceleration in combined mass loss from the Greenland and Antarctic Ice Sheets over the period of the satellite record, 1992–2020.[46] The average Greenland and Antarctic Ice Sheet TMBs over this period were –169 and –92 Gigatonnes per year (Gt·yr^{-1}), respectively, and –261 Gt·yr^{-1} combined. Combining the two ice sheets, the seven highest melt years on record are all since 2010, and average rates of mass loss increased from 105 Gt·yr^{-1} from 1992–1996 to 372 Gt·yr^{-1} from 2016–2020. This is equivalent to ~1 mm·yr^{-1} of global sea level rise attributed to the polar ice sheets in the latter period.
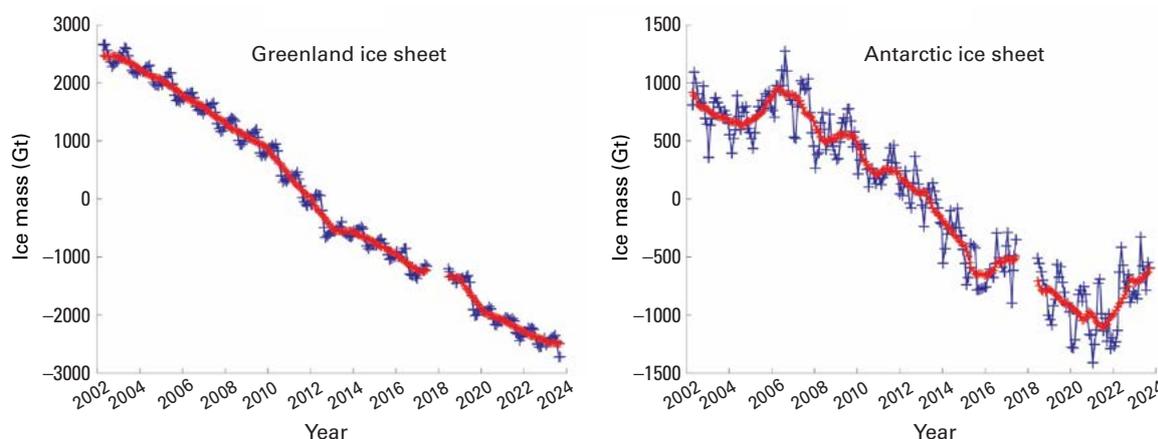
Figure 15. GRACE gravitational mass balance data for the Greenland and Antarctic ice sheets, April 2002 through September 2023.
Source: Data and analysis courtesy of Isabella Velicogna.

Data and modelled estimates of mass balance from 2023 are consistent with these recent rates of mass loss in Greenland, but the Antarctic ice sheet gained mass due to higher-than-normal snow accumulation in the last year and a half (Figure 15). GRACE satellite gravitational data over the 2022-2023 hydrological year 2023 (September 2022 to August 2023) give an estimated mass change of –196 Gt for Greenland, close to the long-term rate of mass loss from the ice sheet. The Antarctic ice sheet gained 122 Gt over this same period.

GLACIERS

Preliminary data indicate the annual mass balance of a global set of reference glaciers for the hydrological year 2022-2023 was –1.2 m w.e. This is nominally the largest loss of ice on record (1950-2023), driven by extremely negative mass balance in both western North America and Europe.

Glaciers in western North America and the European Alps experienced an extreme melt season. In Switzerland, glaciers lost around 10% of their remaining volume in the past two years.

Glaciers are formed from snow that has compacted to form ice, which then deforms and flows downhill. Glaciers comprise two zones: an accumulation zone where accumulation of mass from snowfall exceeds ice loss, and an ablation zone where ice loss (ablation) from melting and other mechanisms exceeds accumulation. Where glaciers end in a lake or the ocean, ice loss can occur through melting where the ice meets the water, and via calving when chunks of the glacier break off.

Glacier mass balance – the amount of mass gained or lost by the glacier – is commonly expressed as the annual thickness change averaged over the glacier area, expressed in metres of water equivalent (m w.e.).[47] Melt rates are strongly affected by the glacier albedo, the fraction of sunlight that is reflected by the glacier surface. Exposed glacier ice is darker and therefore has a lower albedo than the seasonal snowpack and is sensitive to darkening from mineral dust, black carbon, algal activity, and fallout from forest fires. Reduced snow cover, long melt seasons, and wildfire activity all serve to concentrate darker material on the glacier surface, decreasing its albedo and thereby increasing the melt.

Preliminary data from a set of reference glaciers monitored by the World Glacier Monitoring Service (WGMS) indicate a global annual mass balance for the hydrological year 2022–2023 of –1.2 m w.e. that is slightly more negative than 2021–2022 for the set of about 60 WGMS reference glaciers. This is nominally a record low mass balance (1950–2023, Figure 16) based on the available glacier data. The record loss was driven by extremely negative mass balance in both western North America and Europe. Seven out of the ten most negative mass-balance years have occurred since 2010.

The annual mass loss for Swiss glaciers in 2022–2023 was the second largest on record (1950 to present, Figure 17) at 4.4% of the remaining ice volume. Together with the record mass loss in 2021–2022 of 5.9%, Swiss glaciers have lost around 10% of their remaining volume in just two years. This has been driven by low snowpacks and warm summers each year with potential cumulative impacts from glacier darkening associated with longer-than-normal periods of exposed glacier ice and loss of the high-elevation firn.[49]
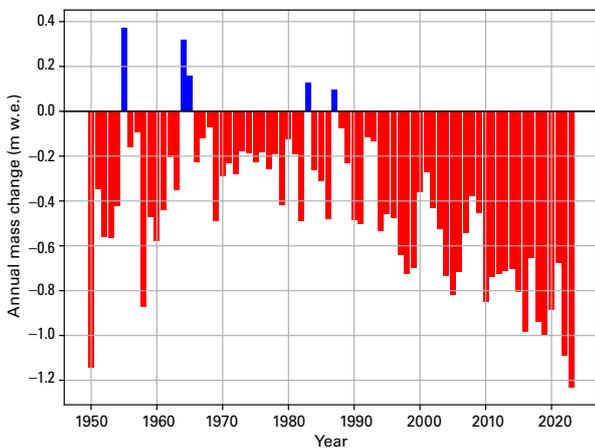
Figure 16. Annual mass balance of reference glaciers with more than 30 years of ongoing glaciological measurements. Annual mass change values are given on the y-axis in the unit meter water equivalent (m w.e.) which corresponds to tonnes per square meter (1 000 kg·m^{-2}).

Source: WGMS (2023, updated and earlier reports)[48]
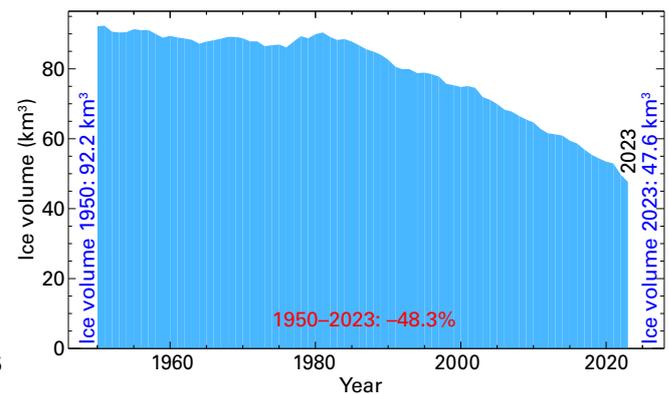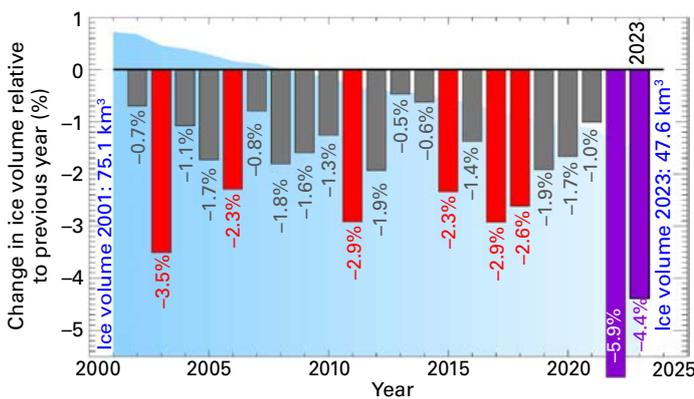
Figure 17. (left) Total annual loss of Swiss glaciers related to the current ice volume. The vertical bars indicate the percentage change in ice volume relative to the previous year. Red and purple bars are the 8 largest relative mass losses on record. The purple bars are the relative mass losses for 2022 and 2023. The blue shaded area in the background represents the overall ice volume as also shown in the right-hand panel. (right) Overall ice volume for Swiss Glaciers 1950-2023.

Source: Matthias Huss based on Glacier Monitoring Switzerland, 2022: Swiss Glacier Mass Balance (Release 2023), https://doi.org/10.18750/massbalance.2022.r2022.
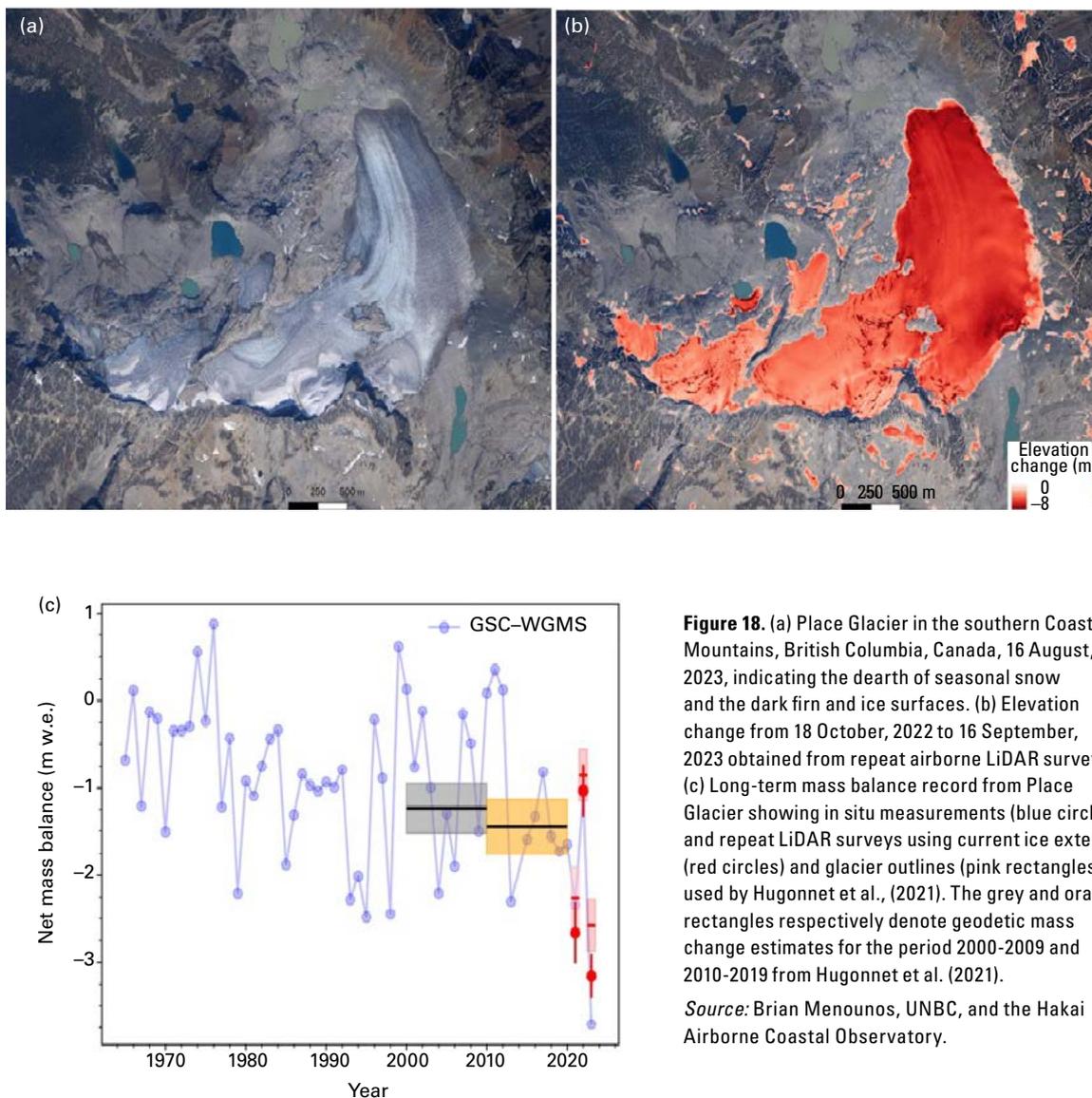
Figure 18. (a) Place Glacier in the southern Coast Mountains, British Columbia, Canada, 16 August, 2023, indicating the dearth of seasonal snow and the dark firn and ice surfaces. (b) Elevation change from 18 October, 2022 to 16 September, 2023 obtained from repeat airborne LiDAR surveys. (c) Long-term mass balance record from Place Glacier showing in situ measurements (blue circles) and repeat LiDAR surveys using current ice extent (red circles) and glacier outlines (pink rectangles) used by Hugonnet et al., (2021). The grey and orange rectangles respectively denote geodetic mass change estimates for the period 2000-2009 and 2010-2019 from Hugonnet et al. (2021).

Source: Brian Menounos, UNBC, and the Hakai Airborne Coastal Observatory.

Western North America experienced record (1965 to present) glacier mass loss in 2023, with glacier-averaged annual thinning of more than 3.5 m at LiDAR-monitored[50] glacier sites in the Canadian Rockies and southern Coast Mountains. Based on regional LiDAR surveys, North American glaciers lost mass at rates that were five times higher than rates measured for the period 2000–2019.[51] Adjusting the LiDAR altimetry data for snow and ice density, estimates of mass balance at two sites with long-term measurements, Place (Figure 18) and Haig Glaciers, are respectively, –3.1 ± 0.5 and –3.8 ± 0.6 m w.e. In situ mass balance measurements from these two sites give estimates of –3.7 and –4.1 m w.e., respectively, far below the long-term mean and more than 1 m w.e. below the previous record minima.

The large negative mass balances are due to a below-average winter snowpack followed by an intense spring heatwave that led to early exposure of bare ice across most glaciers and icefields in southwest Canada. Seasonal snow was mostly gone in mid-summer (Figure 18) on most glaciers, exposing darker firn or ice over an extended melt season. Above-average summer temperatures and record wildfire activity in western Canada[52] (see Extreme weather and climate events) contributed to the extreme melt, with particulate deposition from

the wildfires further darkening the glacier surfaces. High rates of cumulative melting over the past several years may also be a factor, as impurities are increasingly concentrated on the glacier surfaces and the firn zone has been lost on many mountain glaciers. These factors are becoming persistent, and glaciers in western North America have lost an estimated 9% of their 2020 volume over the period 2020–2023.

SNOW COVER

Seasonal snow cover in the Northern Hemisphere has been experiencing a long-term decline in the late spring and summer. Northern Hemisphere snow cover extent for May was the eighth lowest on record (1967–2023). North American snow cover extent for May 2023 was the lowest on record (1967–2023).

Seasonal snow cover in the Northern Hemisphere has been experiencing a long-term decline in the late spring and summer, which continued in 2023. Northern hemisphere snow-cover extent from January through April 2023 was close to the long-term average (1991–2020), but the spring heat wave in north-western North America drove widespread snowmelt. North American snow cover extent for May 2023 was the lowest on record (1967–2023) at 7.47 million km^2, about 1.57 million km^2 (17%) below the long-term average, while overall Northern Hemisphere snow cover extent was 16.74 million km^2, the eighth lowest since 1967, and 1.47 million km^2 below the long-term average (Figure 19).
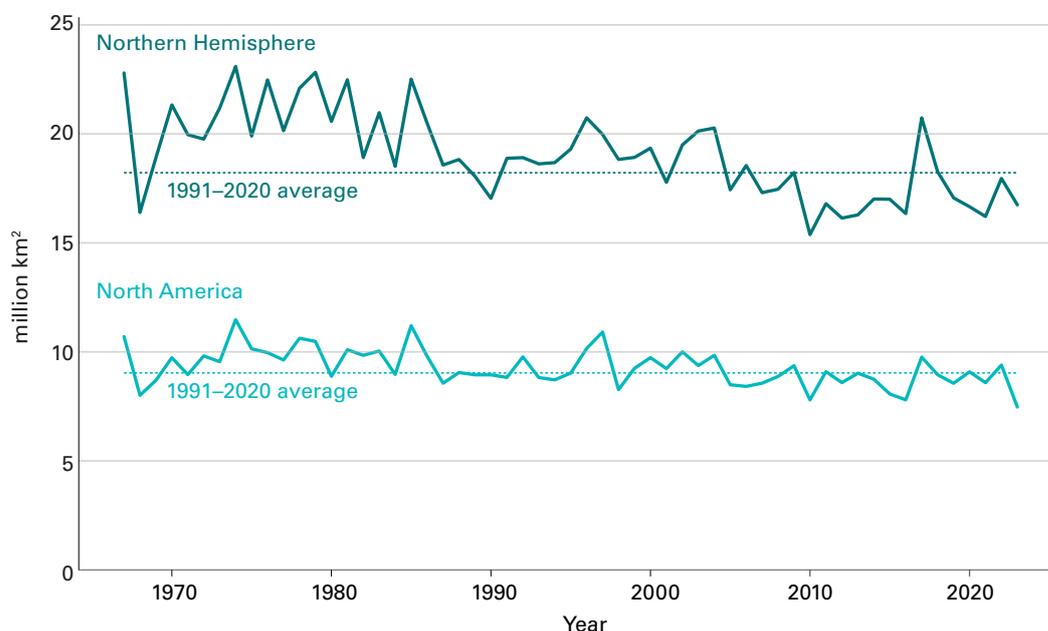

Figure 19. May snow-cover extent for the Northern Hemisphere (dark blue) and North America (light blue), 1967–2023. The 1991–2020 average for each region is shown as a horizontal dotted line.

Source: Data from the Rutgers University Global Snow Lab[53] (https://climate.rutgers.edu/snowcover/).

Climate Monitoring and Renewable Energy

Hamid Bastani and Roberta Boscolo

Renewable energy generation, primarily driven by the dynamic forces of solar radiation, wind and the water cycle, has surged to the forefront of climate action for its potential to achieve decarbonization targets. Worldwide, a substantial energy transition is already underway. In 2023, renewable capacity additions increased by almost 50% from 2022, for a total of 510 gigawatts (GW).[54] Such growth marks the highest rate observed in the past two decades and, as the International Energy Agency (IEA) indicates, demonstrates the potential to achieve the clean energy goal set at COP28 to triple renewable energy capacity globally to reach 11 000 GW by 2030.[55]

In the era of this massive and fast transition to renewables, understanding the critical nexus between climate variability and renewable energy is pivotal. A comprehensive knowledge of how the climate is going to modulate the availability of and demand for renewable energy is essential for optimizing operation, investments and planning of energy resources. The recent joint publication of WMO and International Renewable Energy Agency (IRENA) on *Climate-driven Global Renewable Energy Potential Resources and Energy Demand in 2022* (WMO-IRENA 2023) underscores the inherent links between renewable energy resources and weather and climate conditions. The report emphasizes the potential for developing countries, especially in Africa where energy access remains a key priority, to develop clean energy systems and urges better accounting for climate variability for improved operation, management and planning of energy resources.

The importance of accounting for climate variability can be seen in Figure 21, which shows monthly energy supply and demand anomalies in Botswana, Mozambique, Namibia, South Africa, and Zimbabwe in 2022 relative to the average of the 1991-2020 reference period. The anomalies are measured by four defined energy indicators, which are capacity factors[56] for wind power (WP), Solar PV (SPV), Weighted total precipitation (WTP) as a hydropower proxy indicator, and Energy Degree Days (EDD) as a proxy for energy demand indicator.
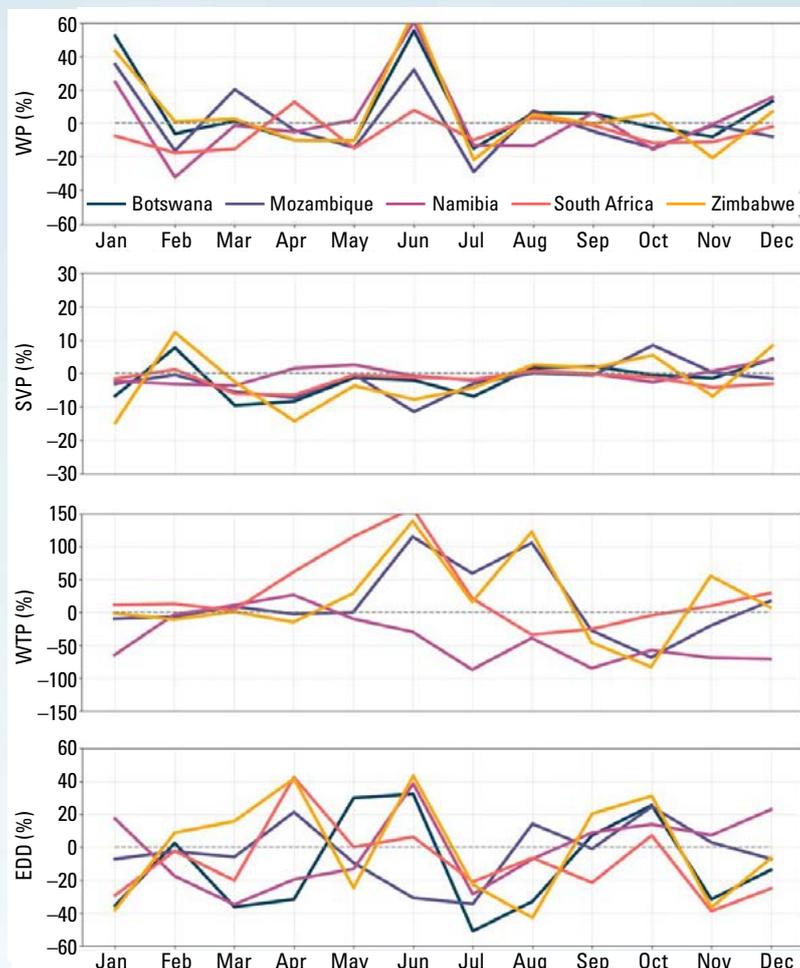
To illustrate how the plots can be interpreted, consider October when demand in all five countries is between 5% and 30% higher than average, while a large portion of potential generation is lower than average (except for small increases in SPV for Mozambique and Zimbabwe, and WP for Zimbabwe). In this situation, balancing power would require careful planning, for instance to ensure there is enough water in hydropower dams from the previous rainy season (typically ending in May), and ahead of the next rainy season (typically starting in October–November).

For more detailed information about the indicators and additional insights on other regions and global results, refer to the main publication.[57]

Figure 20. Monthly percentage anomalies of four energy indicators for wind power (WP), solar PV (SPV), hydropower (WTP) and energy demand (EDD) for 2022 relative to corresponding months in the 1991-2020 reference period for five countries in Southern Africa as indicated in the legend of the top panel. Note that Botswana does not have hydropower plants, and therefore no indicator has been computed. Also note that the y-axis varies depending on the range of the indicator.

STRATOSPHERIC OZONE AND OZONE-DEPLETING GASES

Following the success of the Montreal Protocol, use of halons and Chlorofluorocarbons (CFCs) has been reported as discontinued but their levels in the atmosphere continue to be monitored.[58] Because of the long lifetimes of CFCs, these compounds will remain in the atmosphere for many decades and, even if there were no new emissions, there would still be more than enough chlorine and bromine present to cause complete destruction of ozone in Antarctica from August to December. As a result, the formation of the Antarctic ozone hole continues to be an annual spring event with year-to-year variation in its size and depth governed to a large degree by meteorological conditions. The "hole" is not strictly speaking a hole; it is an area where the total column ozone in the stratosphere falls below 220 Dobson units.[59]

In 2023, the development of the ozone hole had an unusually early start, becoming the 6th largest in the satellite era. It expanded to 26 million km^2 on 21 September, comparable with the two previous years (2021 and 2022) and close to the maxima observed in earlier years such as 28.2 million km^2 in 2015 and 29.6 million km^2 in 2006 according to analyses from the National Aeronautics and Space Administration[60] (NASA) and Copernicus Atmospheric Monitoring Service[61] (CAMS). NASA reported a minimum ozone of 99 DU on 3 October 2023. Despite the area of the ozone hole decreasing in a typical manner through early October, it increased again towards the end of the month and remained at or above approximately 15 million km^2 until the first week of December. Although the ozone hole was unusually long-lived in 2023, its longevity was similar to that of the ozone holes of the last three years.
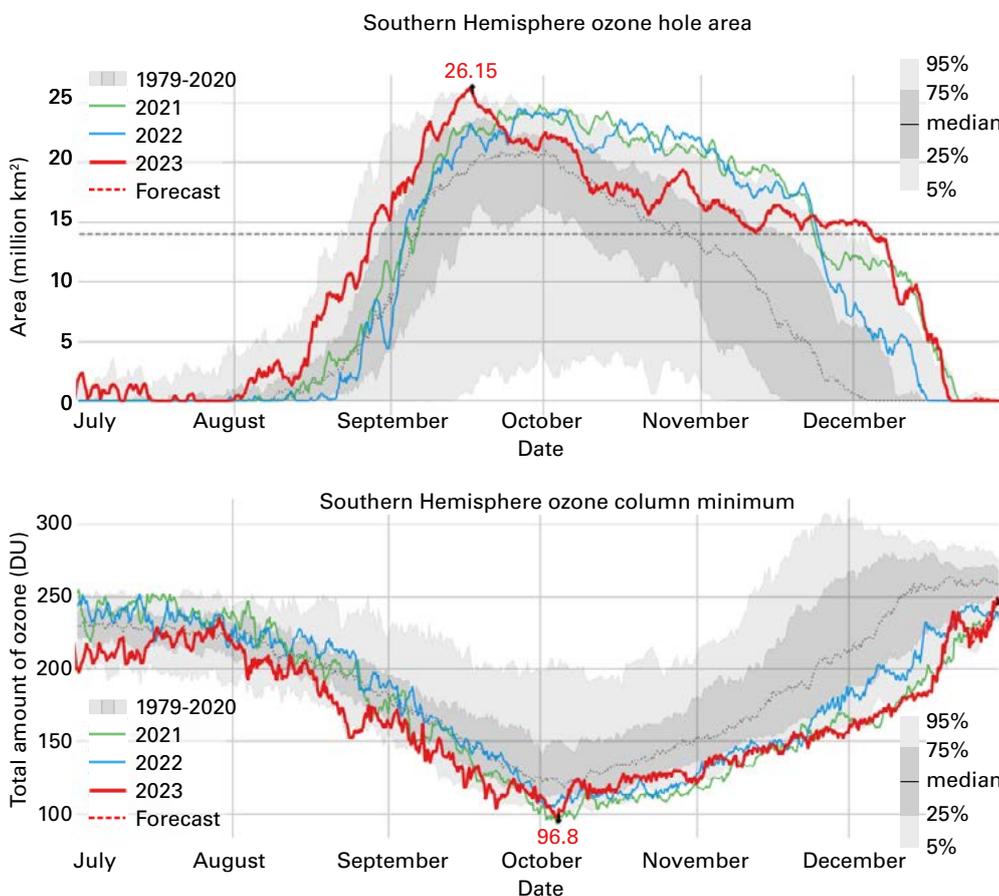

Figure 21. Area (millions of km^2) and Minimum Ozone where the total ozone column is less than 220 Dobson units; 2023 is shown in red. The three most recent years are shown for comparison as indicated by the legend. The smooth, thick grey line is the 1979–2020 average.

Source: The plot is produced by Copernicus Atmosphere Monitoring Service.

The unusual persistence of the ozone holes in the past three years was due to below-average stratospheric temperatures and a strong polar vortex lasting until December. Several potential drivers for the observed stronger polar vortex have been identified, including water vapor injected into the stratosphere by the eruption of Hunga Tonga–Hunga Ha'apai, wind patterns in the Southern Hemisphere, and climate change.

SHORT-TERM CLIMATE DRIVERS

A prolonged period of La Niña from mid-2020 to early 2023 gave way to El Niño conditions which were well established by September 2023, contributing to the observed rise in global mean sea-surface temperatures during 2023.

There are many different natural phenomena, often referred to as climate patterns or climate modes, that affect weather and climate at timescales ranging from days to several months or even years. In 2023, the El Niño–Southern Oscillation (ENSO), the Indian Ocean Dipole, and the North Atlantic Oscillation, highlighted here, contributed to major weather and climate events across large areas of the world.

ENSO – EL NIÑO SOUTHERN OSCILLATION

ENSO is one of the most important climate drivers of year-to-year variability in weather patterns worldwide. It is linked to hazards such as heavy rains, floods, and drought, heatwaves, and cold spells. El Niño, characterized by higher-than-average sea-surface temperatures in the eastern tropical Pacific and a weakening of the trade winds, typically has a warming influence on global temperatures. La Niña, which is characterized by below-average sea-surface temperatures in the central and eastern tropical Pacific and a strengthening of the trade winds, has the opposite effect.

A multi-year La Niña event began in mid-2020 and ended in early 2023. Subsequently, sea-surface temperatures in the eastern tropical Pacific increased, crossing typical El Niño thresholds (0.5 °C in Figure 22) by June. However, the atmosphere was slower to respond, and it was not until early September that El Niño conditions were well established in both the atmosphere and ocean. By the end of the year, a strong El Niño had developed, with the Oceanic Niño Index reaching 2.0°C for the November-January period, the highest value since the 2015/16 El Niño.
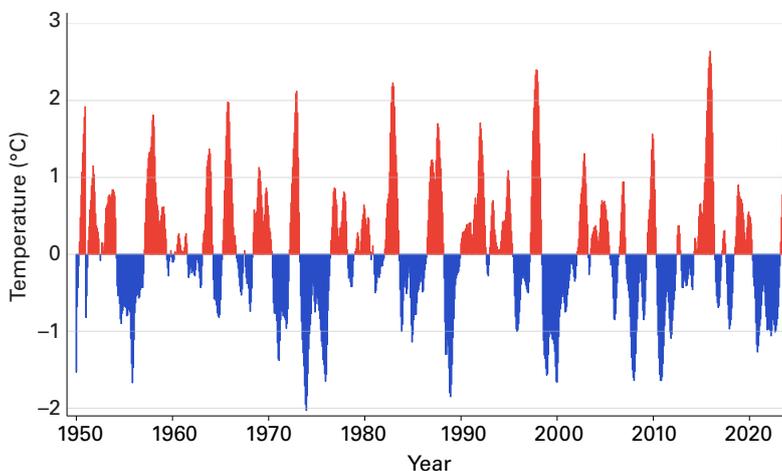
Figure 22. Time series of NOAA's Oceanic Niño index from January 1950 to December 2023 showing the presence of cooler-then-average conditions (blue) and warmer-than-average conditions (red) during 3-month average time periods. Anomalies are with respect to the 1991–2020 average sea-surface temperature.

Source: NOAA NCEP

El Niño has an influence on regional rainfall patterns. Precipitation anomalies were typical of El Niño in some regions: drier than usual conditions in maritime Southeast Asia and from southern Mexico to northern South America and wetter than normal conditions in parts of Chile (Figure 23).

Decreased monsoon rainfall in southeast Asia is associated with El Niño. Onset of the monsoon over Kerala, India, occurred on 8 June, 7 days later than normal. By the end of September, India had received 94% of its typical monsoon rainfall.[62] Higher than normal rainfall totals, however, were observed along the lower course of the Indus River and in central India.

In Australia, La Niña is associated with wetter-than-normal conditions and El Niño with drier-than-normal conditions. In January, rainfall for the country was 35% above normal as La Niña wound down, but in August it was 50% below normal with a strengthening El Niño. The dryness was also accompanied by the highest July-to-September national mean temperatures in Australia's 114-year record. September was the driest on record in Australia and August to October was the driest three-month period in the 124-year observational record. However, somewhat atypically for an El Niño event, November and December were wetter than average in much of eastern Australia.

As average global temperature anomalies increased during the transition from La Niña to El Niño, many regions also experienced heatwaves, including parts of the United States, Mexico, Europe, North Africa and the Middle East, China, Siberia, and South America. A UNEP Frontiers report[63] highlighted that variability associated with El Niño has implications for biomass and fire weather[64] which increases the risk of large and intense wildfires in some places. Please refer to the section on Extreme weather and climate events for more details on extreme events.

IOD – INDIAN OCEAN DIPOLE

The positive phase of the IOD is characterised by below-average sea-surface temperatures (and sea level) in the eastern Indian Ocean and above average sea-surface temperatures (and sea level) in the west. The negative phase has the opposite pattern. The resulting change in the gradient of sea-surface temperature across the ocean basin affects the weather of the surrounding continents, primarily in equatorial regions and the Southern Hemisphere. Positive IOD events are often, but not always, associated with El Niño and negative events with La Niña.

In conjunction with the emergence of El Niño, the first positive IOD since 2019 developed in early austral spring and peaked during October. The positive IOD helped to intensify the anomalously dry and warm conditions over parts of Australia during this time. Conversely, rainfall totals in the Horn of Africa during the October–December rainy season were much higher than normal, leading to flooding in Somalia, Ethiopia, and Kenya; this follows the prolonged drought in the region from 2020 to early 2023 when La Niña conditions and a neutral to negative Indian Ocean dipole were largely present.

NAO – NORTH ATLANTIC OSCILLATION

Average sea level pressure in the North Atlantic is characterized by an area of lower pressure close to Iceland known as the Icelandic Low and an area of higher pressure centred over the Azores known as the Azores High. The North Atlantic Oscillation (NAO) is based on the sea-level pressure difference between the Icelandic Low and the Azores high. It is mainly associated with driving weather conditions in the North Atlantic basin, Europe, and the Mediterranean. The positive phase is characterized by below-normal pressure over the North Atlantic high latitudes and above-normal pressure over the central Atlantic, the eastern United States,

and western Europe. The negative phase has the opposite pattern. Because the phases are determined by pressure changes in the atmosphere, they can fluctuate more rapidly, on the order of days to weeks, compared with other climate drivers such as ENSO, which are driven by slower changes in ocean temperature and fluctuate on the order of months to years.

High pressure associated with the negative NAO in late June and July 2023 contributed to a heatwave that caused significant snow and ice melt across southern Greenland. Several widespread melting events occurred during this period. Ireland reported its warmest June on record (124 years), as did the long-running Uccle station in Belgium (191 years). In eastern Canada, many locations reported record warmth for July.

PRECIPITATION

Accumulated precipitation totals in 2023 were above the long-term average (Figure 23) in East and Central Asia and parts of northern Asia; the western Indian summer monsoon region; parts of the Maritime Continent; northern New Zealand; parts of West, Central, Southern and East Africa; West, Central and Southeast Europe; southern Scandinavia; the western Middle East; northwest, southwest and southeast North America; Greater Antilles; and parts of southeast South America.

Regions with a marked rainfall deficit included: southeast South America, the Amazon Basin, and much of Central America; southern Canada; the western Mediterranean region and Southwest Europe; parts of northwest, central, and southern Africa; parts of central Asia; the eastern Indian Monsoon region; parts of southeast Asia and the Maritime Continent; southwest and coastal north Australia; and many of the Pacific Islands.

The onset of the West African Monsoon was around normal. The Greater Horn of Africa region, which had been experiencing long-term drought, suffered substantial flooding in 2023, particularly later in the year as heavy rains associated with El Niño and the positive Indian Ocean Dipole became established (see Extreme weather and climate events).
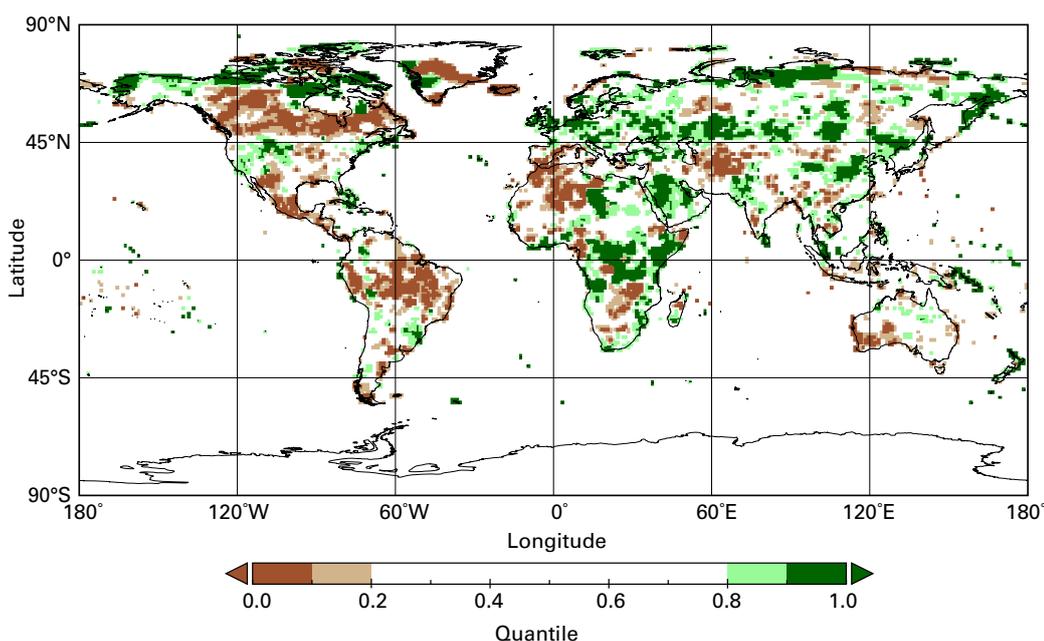
Figure 23. Total precipitation in 2023, expressed as a quantile of the 1991–2020 reference period, for areas that would have been in the driest 20% (brown) and wettest 20% (green) of years during the reference period, with darker shades of brown and green indicating the driest and wettest 10%, respectively.

Source: Global Precipitation Climatology Centre (GPCC), Deutscher Wetterdienst, Germany). For more details see Data sets and methods.

Extreme weather and climate events

Extreme weather continues to lead to severe socio-economic impacts.

Extreme heat affected many parts of the world.

Wildfires in Hawaii, Canada and Europe led to loss of life, the destruction of homes and large-scale air pollution.

Flooding associated with extreme rainfall from Mediterranean Cyclone Daniel affected Greece, Bulgaria, Türkiye, and Libya with particularly heavy loss of life in Libya.

Extreme weather and climate events had major impacts on all inhabited continents in 2023. These included major floods (some of them associated with tropical cyclones), extreme heat and drought, and associated wildfires which presented challenges to water and food security as well as human welfare.[65,66] Some of the most significant events are described below, with a broader range of events described in the online supplement.

One of the most significant single weather-related events in terms of loss of life was the Mediterranean Cyclone (or *medicane*) referred to locally as Storm *Daniel* in September. In its initial stages, the storm produced extreme rainfall in Greece, southern Bulgaria, and parts of Türkiye, while at the same time another storm system produced significant flash flooding in Spain with adverse effects on cereal production.[67] The heaviest falls were in the Thessaly region of Greece north of Athens, where Zagora Pelion received 760 mm on 5 September and a 5-day total of 1096 mm from 4 to 8 September, while in Bulgaria, 329 mm fell in 16 hours at Kosti on 4–5 September. The storm then remained slow-moving in the eastern Mediterranean for several days before its major rainbands impacted north-eastern Libya on 10 and 11 September. Extreme rainfalls affected the coast and nearby mountains, with 414 mm falling in 24 hours at Al-Bayda on 10–11 September. The intense rainfalls resulted in extreme flooding in the region. The most extreme impacts were in the city of Derna (about 50 km east of Al-Bayda), where much of the central city was destroyed by flooding that was exacerbated by the failure of two dams. At least 4 700 confirmed deaths in Libya[68] have been attributed to the flooding, with 8 000 people still missing (as of 15 December). There were 19 additional deaths in Greece[69] and Bulgaria.

Tropical Cyclone *Freddy* in February and March was one of the world's longest-lived tropical cyclones. It formed on 6 February off the western coast of Australia and, after earlier landfalls in Madagascar and Mozambique, made its final landfall in Mozambique on 11 March before moving inland as a remnant low. The major impacts of *Freddy* came because of flooding during the final landfall, both in Mozambique and Malawi, as extremely heavy rain fell (up to 672 mm during the storm in Mozambique). Parts of Mozambique and Malawi had not yet recovered from storms in 2022. Malawi was especially hard hit with at least 679 deaths reported and over 659 000 internal displacements[70], with a further 165 deaths in Mozambique.[71] Casualties were also reported in Madagascar and Zimbabwe, and at sea near Mauritius.

Tropical Cyclone *Mocha*, in May, was one of the most intense cyclones ever observed in the Bay of Bengal, reaching peak 10-minute sustained winds of 115 kt. It formed on 11 May and made landfall near the Bangladesh-Myanmar border on 14 May.[72] In Bangladesh, displacement was reported in Cox's Bazar, the world's largest refugee settlement, which is home to over 900 000 Rohingya refugees from Myanmar.[73] More than 29 000 people were temporarily relocated.[74] In total at least 156 lives were lost in Myanmar[75] and over 270 000 buildings damaged or destroyed.[76] At least 63 000 displacements took place in camps sheltering people already displaced by conflict and violence.[77] The effects of Cyclone *Mocha*, together with an intensification of conflict and record high food prices, have severely aggravated acute food insecurity, especially among the 3.4 million vulnerable people assessed as in need of humanitarian assistance.[78]

The largest reported economic loss from a single event in 2023 was from Hurricane *Otis*, which hit the Pacific coast of Mexico in late October. Otis reached hurricane intensity at 1200 UTC on 24 October, and within fifteen hours had intensified to a category 5 system,[79] one of the most

rapid rates of intensification observed in the satellite era. Shortly afterwards, it made landfall just west of Acapulco at near peak intensity, with maximum sustained winds of 260 km·hr^{-1}, which might be the first known category 5 landfall on the Pacific coast of Mexico. The hurricane caused widespread destruction in Acapulco and surrounding areas, with economic losses estimated at around US$12 billion.[80] At least 48 deaths were attributed to the hurricane[81] with a further 32 missing, mostly at sea.

The North Island of New Zealand suffered repeated extreme rainfall and flooding events in January and February. The most significant was on 13–14 February, when Cyclone *Gabrielle* passed just east of the North Island as a post-tropical system. Daily rainfalls exceeded 500 mm in parts of the eastern North Island and Auckland (971.5 hPa) had its lowest air pressure on record. 11 deaths were reported because of *Gabrielle* and 4 from more localized floods in Auckland on 27–28 January. Total economic losses from the two events were estimated at US$5.3 to 8.6 billion[82], by far the costliest non-earthquake disaster recorded in New Zealand.

Many significant heatwaves occurred in various parts of the world during 2023. Some of the most significant were in southern Europe and North Africa, especially in the second half of July where severe and exceptionally persistent heat occurred. Italy was particularly affected, with temperatures reaching 48.2 °C on 24 July at the Sardinian sites of Lotzorai and Jerzu, only 0.6 °C below the European record set in Sicily in 2021.[83] On 23 August, a mean daily temperature of 32.98 °C was reported at the Brera Observatory in Milan, the highest in a record dating back to 1763. Among the locations experiencing record high temperatures were Tunis (Tunisia) (49.0 °C on 24 July), Tirana (Albania) (43.0 °C on 25 July), Agadir (Morocco) (50.4 °C on 11 August), and Algiers (49.2 °C on 23 July). The extreme heat shifted to southeast Europe in late July, and there were further heatwaves affecting west-central Europe in late August and early September. Numerous locations in southern France, northern Spain and western Switzerland set records during these events, including Toulouse (42.4 °C on 23 August[84]). There was also extensive wildfire activity during the summer, particularly in Greece (both on the mainland and islands). A fire in north-eastern Greece in late August and early September that burned 96 000 hectares was the largest fire ever observed in the European Union.[85]

Canada's wildfire season was well beyond any previously recorded. Significant fire activity began in late April, expanded during a very warm, dry May, and continued throughout the summer and into early autumn. The total area burned nationally for the year was 14.9 million hectares, more than seven times the long-term average (1986–2022) and far above the previous record seasonal total of 6.7 million hectares in 1989 (Figure 24). 297 evacuation orders were
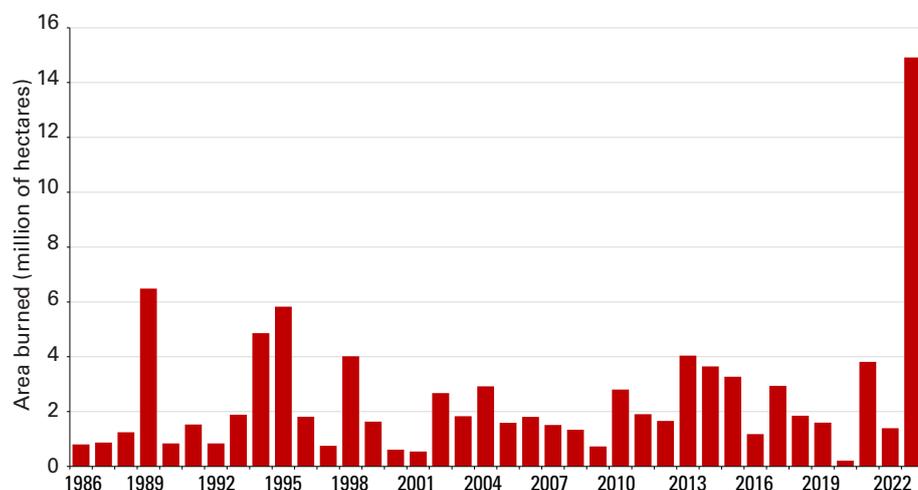

Figure 24. Annual Area Burned in Canada 1986–2023 (millions of hectares).

Source: Jain et al. (2024)[87]

issued, for over 235 000 people.[86] The fires also resulted in significant and widespread smoke pollution, particularly in the heavily populated areas of eastern Canada and the north-eastern United States in the first half of June. Four deaths were directly attributed to fires, although the broader health impacts of the smoke are yet to be fully assessed.

The deadliest single wildfire of the year occurred in Hawaii, on the western side of the island of Maui. Extreme fire weather conditions, with low humidity and strong, gusty winds driven by a pressure gradient between strong high pressure to the north and the circulation of Hurricane *Dora* well to the south, combined with pre-existing drought to favour the development and rapid spread of intense fires. The most affected region was around the town of Lahaina, which was largely destroyed with over 2 200 structures lost. Mandatory evacuation notices were issued for 7 500 people across the area.[88] At least 100 deaths were reported,[89] the most in a wildfire in the United States for more than 100 years, with 400 homes destroyed.[90] Wildfires of such intensity and speed of movement are extremely rare in the tropics.

Long-term drought persisted in north-western Africa and parts of the Iberian Peninsula, as well as parts of central and southwest Asia, and intensified in many parts of Central America, northern South America and the southern United States. Among the most significant areas of drought was an area of subtropical South America, focused on northern Argentina and Uruguay. Rainfall from January to August was 20 to 50% below average over much of northern and central Argentina, with some regions experiencing their fourth successive year of significantly below average rainfall. In Uruguay, water storages reached critically low levels, badly affecting the quality of supplies to major centres including Montevideo, although there was some improvement in the situation from August. Although there was some easing of drought conditions in subtropical South America later in the year, drought intensified in many parts of the continent's interior, including large parts of the Amazon basin. Eight Brazilian states recorded their lowest July to September rainfall in over 40 years. The Rio Negro at Manaus reached a record low (observations started in 1902) level on 26 October, 0.93 m below the previous record set in 2010.[91]

The Greater Horn of Africa region, which had been experiencing long-term drought, suffered substantial flooding in 2023, particularly later in the year following heavy rains associated with El Niño and the positive Indian Ocean Dipole (see Short-term climate drivers). The most badly affected area was the region encompassing the southern half of Somalia, southeastern Ethiopia and northeastern Kenya. During the Deyr rainy season (October and November), monthly rainfall in this region was widely 100 to 200 millimetres and locally exceeded 200 millimetres, several times the long-term averages. There were at least 352 deaths reported across the three countries.[92] Across Ethiopia, Burundi, South Sudan, Tanzania, Uganda, Somalia and Kenya, widespread and severe flooding displaced 1.8 million people[93] in addition to the 3 million people displaced internally or across borders by the five consecutive seasons of drought[94] in Ethiopia, Kenya, Djibouti, and Somalia. The wet conditions did lead to some recovery in pasture and crop conditions after the extended drought. Landslides and flooding in early December also resulted in at least 89 deaths in northern parts of the United Republic of Tanzania.[95] Pastoralist communities have continued to be affected by asset losses after two consecutive years of drought. These continued to adversely affect agricultural production and reduced cereal production in 2023 compared to 2022.[96]

Socio-economic impacts

Food security, population displacements and impacts on vulnerable populations continue to be of mounting concern in 2023, with weather and climate hazards exacerbating the situation in many parts of the world.

Extreme weather and climate conditions continued to trigger new, prolonged, and secondary displacement in 2023 and increased the vulnerability of many who were already uprooted by complex multi-causal situations of conflict and violence.

Development and implementation of local disaster risk reduction strategies have increased since the adoption of the Sendai Framework for Disaster Risk Reduction.

One of the essential components for reducing the impact of disasters is to have effective multi-hazard early warning systems.

The events described above, and many others besides, occur in a broader context. Extreme weather and climate events interact with and in some cases trigger or exacerbate situations concerning water and food security, population mobility and environmental degradation.[97,98]

FOOD SECURITY

The number of people who are acutely food insecure worldwide has more than doubled, from 149 million people before the COVID-19 pandemic to 333 million people in 2023 (in 78 monitored countries by WFP).[99] Global hunger levels remained unchanged from 2021 to 2022. However, these are still far above pre-COVID-19 pandemic levels: in 2022, 9.2% of the global population (735.1 million people) were undernourished, compared to 7.9% of the population (612.8 million people) in 2019 (Figure 25).[100] The current global food and nutrition crisis is the largest in modern human history.[101] Protracted conflicts, economic downturns, and high
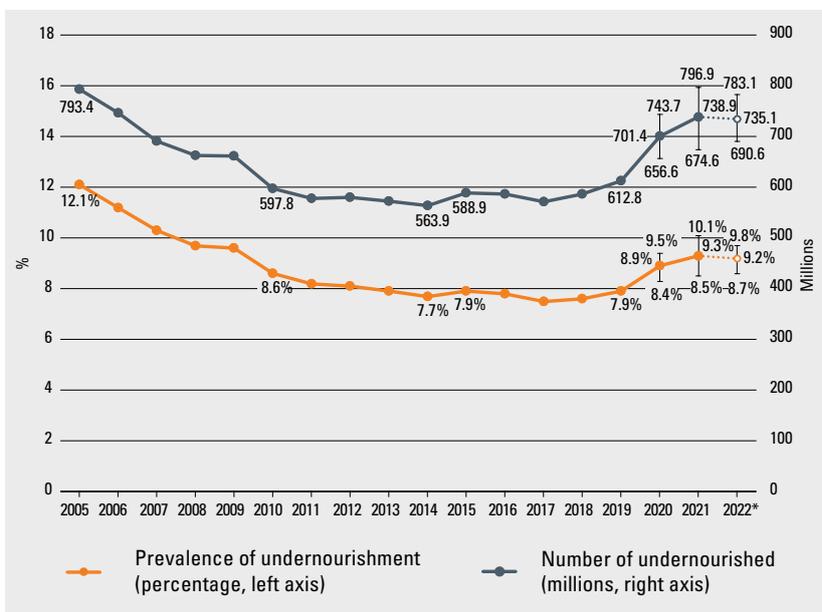

Figure 25. Global prevalence of undernourishment (as a%) and number of undernourished (in millions) since 2005.

Source: The entire series was updated to reflect new information released since the publication of The State of Food Security and Nutrition in the World 2023.[103]

food prices, further exacerbated by high costs of agricultural inputs driven by ongoing and widespread conflict around the world, are at the root of high global food insecurity levels. This is aggravated by the effects of climate and weather extremes. In southern Africa, for example, weather extremes, including the passage of Cyclone *Freddy* in February 2023, have affected areas of Madagascar, Mozambique, southern Malawi, and Zimbabwe. Flooding associated with the cyclone submerged extensive agricultural areas and inflicted severe damage on crops. This has exacerbated a slow economic recovery.[102]

Globally, annual economic losses from climate and weather-related disasters have increased since the 2000s.[104] Between 2007 and 2022, 88 post-disaster needs assessment surveys conducted in 60 countries worldwide showed that over 65% of losses caused by droughts occurred in the agriculture sector, including crop and livestock production losses. For floods, storms, and cyclones, around 20% of losses are in agriculture.[105]

In early 2023, South Sudan continued to experience exceptional flooding, with water levels remaining high even during the dry season. Even with relatively dry conditions locally, flooding persisted due to high flows from further upstream in the Nile basin, and very slow drainage from earlier floods. The prolonged flooding made it difficult for people to access basic needs such as food, clean water, and healthcare and contributed to the near collapse of local livelihoods. Between April and July 2023, 7.8 million people, almost two-thirds of the total population in South Sudan, were expected to experience severe acute food insecurity.[106]

Afghanistan experienced a substantial reduction in snowmelt and rainfall, resulting in another poor crop season. This led to widespread acute food insecurity, particularly in the north and northeastern regions. Between May and October 2023, 15.3 million Afghanis were estimated to face severe acute food insecurity[107]. In Yemen, 53% of the population were already classified as in a *crisis* level of acute food insecurity or worse between October and December 2022. High food and fuel prices, together with floods from March to September 2023, and protracted conflict, have further aggravated food insecurity.

In Indonesia, a meteorological drought linked to El Niño and the positive phase of the Indian Ocean Dipole (see Short-term climate drivers) occurred during the dry season, affecting 23 450 hectares of paddy cultivation, and causing 6 964 hectares of crop failure, as of August 2023. A decrease of 645 000 tonnes of rice production was predicted by October 2023.[108] Crop planting in late 2023 was also delayed.

In 2023, a record maize production in Brazil compensated for below-average harvests elsewhere in South America due to prolonged dry spells, especially in Argentina where drought conditions are expected to result in a 15% decrease in cereal production compared to the five-year average. The return of El Niño in 2023 led to adverse consequences through the entire crop cycle of maize in Central America and northern parts of South America, where water deficits and high temperature have curtailed both planting area and yields with compounding negative impacts on final production particularly for the small-holders and more vulnerable households in the *Corredor Seco*. During the second part of the season, tropical storms and unexpected heavy rain events have disrupted the normal growth of crops in certain areas near the Central America Pacific coast. In Haiti, irregular seasonal rainfall including periods of high-intensity precipitation has contributed to decrease the production of primary crops.[109]

Oceania is expected to experience the sharpest annual reduction rate on cereal production worldwide, with a 31.1% decline in 2023 compared to 2022, although this largely reflects a reversion to near-average conditions after exceptionally high production in 2022, with 2023 only slightly below 5-year averages.[110]

In September, Storm Daniel brought heavy rainfall to the coastal and northeastern Libya, flooding nearly 3 000 hectares of cropland, particularly in the Almarj and Derna regions. These constitute the main cropland areas in the eastern part of the country and key sources of livelihoods. The collapse of dams in Derna affected the irrigation system and the floods affected many parts of the agrifood value chain, damaging roads, cereal storage, and overall market channels. According to the FAO's Global Information and Early Warning System (GIEWS) Libya was already in a state of food crisis and in need of external assistance in July 2023 before the floods.[111]

DISPLACEMENT

Across the globe, millions of people, including internally displaced persons, refugees, and migrants, are on the move or have been forced to flee their homes and communities because of disasters exacerbated by climate stresses and shocks. Weather hazards continued to trigger new, prolonged, and secondary displacement in 2023 and increased the vulnerability of many who were already uprooted by complex multi-causal situations of conflict and violence. These trends are a clear indication of how vulnerability to climate shocks and stresses is undermining resilience and creating new protection risks, which threaten the achievements of the SDGs.

An estimated 3.4 million refugees and internally displaced people (IDP) in Syria, Lebanon, Jordan, Iraq and Egypt were in need of critical assistance to cope with the extreme winter conditions in 2023.[112] In northwestern Syria, snowstorms and floods triggered displacements between January and March, many of which were repeated movements of people already displaced by the country's long-running conflict. Similarly, in Yemen, heavy rains hit the country in April. Some IDP sites in Marib Governorate were damaged, leaving dozens of people dead and injured.[113]

Many migrants entering into Somalia found themselves stranded in June and July 2023, mostly in the city of Bossaso, the main coastal crossing location to Yemen, as they were waiting for more favourable weather conditions to cross the Gulf of Aden. In Hargeisa, a group of migrants in transition suffered from extreme heat, and some died from dehydration.[114]

In addition to new displacements caused by high-impact disasters in 2023, many are still enduring the prolonged effects of climate-related displacement that took place in previous years. In Pakistan, the 2022 monsoon floods, which triggered the largest disaster displacement event in a decade, continued to have longstanding impacts in 2023. Displaced communities were still recovering when heavy rains hit some districts in June 2023, causing waterborne and vector-borne diseases.[115]

Displacement in the context of climate change and environmental degradation is often multicausal. Most people move due to a combination of social, political, economic, environmental, and demographic drivers, all of which are and will be affected by climate and environmental change. In Somalia alone, some 531 000 displacements were recorded related to the ongoing drought in 2023 in addition to 653 000 displacements primarily caused by conflict.[116] Subsequent flooding during the October to December rainy season affected more than 2.4 million individuals, displacing more than a million people.[117] Displacement estimates for Storm Daniel indicate close to 45 000 individuals displaced in northeastern Libya.[118] Additionally, a substantial number of migrants were reported to be living in a low-lying area adjacent to the valley, raising concerns that the floods may have destroyed many of their settlements with significant loss of life.[119]

Climate related shocks and stresses in migration and displacement contexts affect people's livelihoods which entrenches poverty (SDG 1) and hunger (SDG 2), pose direct threats to their lives and well-being (SDG 3), widen inequality gaps (SDG 10), limit access to quality education (SDG 4), water and sanitation (SDG 6) as well as clean energy (SDG 7). Women and girls are among the worst affected (SDG 5) due to pre-existing gender and socio-economic inequalities compounding their vulnerabilities.[120]

To better prepare for these contexts, governments, communities, civil society, and the UN are engaged at all levels to strengthen climate resilience and effective disaster risk reduction. A main priority is the community level, where preparedness efforts including early warning systems and emergency preparedness are picking up pace.[121] With 126 countries in possession of disaster risk management strategies and a total of 99 countries reporting to have local governments with disaster risk reduction strategies, development and implementation of local disaster risk reduction strategies have increased since the adoption of the Sendai Framework for Disaster Risk Reduction in 2015.[122]

One of the essential components for reducing the impact of disasters is to have effective multi-hazard early warning systems, and to have effective systems in place for generating disaster risk information, creating early warnings, and disseminating them, as well as having plans to act on the warnings. As of 2023, 102 countries have reported having multi-hazard early warning systems in place, more than half of the countries in the world. The Early Warnings for All initiative was launched by the UN Secretary-General in March 2022 with the aim of ensuring that everyone on Earth is protected from hazardous weather, water, or climate events through life-saving early warning systems by the end of 2027.

The State of Climate Finance

Climate Policy Initiative

In 2021/2022,1 global climate flows reached almost USD 1.3 trillion, nearly doubling compared to 2019/2020 levels. This increase was primarily driven by a significant acceleration in mitigation finance, up by USD 439 billion from 2019/2020. The remainder of the observed growth in 2021/2022 stems from methodological improvements to, and additional data sources used in, the *Global Landscape of Climate Finance*. Despite this growing momentum in climate finance, tracked flows represent only approximately 1% of global GDP.

Comparing tracked climate finance flows to estimated climate finance needs exposes a large financing gap. In an average scenario,[2] for a 1.5°C pathway, annual climate finance investments need to grow by more than six times, reaching almost USD 9 trillion by 2030 and a further USD 10 trillion through to 2050.

Despite the large financing gap, the cost of inaction3 is even higher. Aggregating over the period 2025-2100, the total cost of inaction is estimated at USD 1,266 trillion; that is, the difference in losses under a business-as-usual scenario[4] and those incurred within a 1.5°C pathway. This figure is, however, likely to be a dramatic underestimate of the true cost of inaction, since it does not capture losses to nature and biodiversity, and those induced by conflict and migration, among others. Indeed, the cost of inaction only promises to rise with insufficient mitigation and inadequate adaptation.

Disaggregating global climate finance flows reveals that growth is neither sufficient nor consistent across sectors and regions. The growth in global climate finance in 2021/2022 largely stemmed from significant increases in clean energy investments in only a handful of geographies; China, the USA, Europe, Brazil, Japan and India together received 90% of the increase in funds. Other regions, including many climate-vulnerable countries, and other important sectors – for example, *agriculture* and *industry* – are being left behind, receiving little finance that is disproportionately low given their significant mitigation potential. In addition, emerging mitigation technologies, including battery storage and hydrogen, are only beginning to attract private finance and yet to be scaled-up.

Of particular concern, adaptation finance continues to lag. Though adaptation finance reached an all-time high of USD 63 billion in 2021/2022, the global adaptation financing gap is widening, falling well short of the estimated USD 212 billion per year needed up to 2030 in developing countries alone. Tracked adaptation finance remains dominated by public actors (98%) while tracking challenges continue to impede a clear picture of adaptation

---

[1] CPI reports a biennial average to smooth out fluctuations in the (annual) data.

[2] Climate finance needs are estimated as a range, including lower bound, upper bound, and average needs, based on direct investments in climate-specific physical assets and excluding transition-related unabated fossil fue finance.

[3] Failure to stay within a 1.5°C pathway; for further details see CPI, 2024. The Cost of Inaction. Available at: https://www. climatepolicyinitiative.org/the-cost-of- inaction/#:~:text=CPI's%20estimate%20of%20USD%201%2C266,%2C%20 warming%20scenarios%2C%20and%20timeframes

[4] Equivalent to a 3°C pathway.

action by the private sector. The majority of adaptation finance is directed to the *water and wastewater* sector, reflecting efforts to build resilience to water stress, while other sectors with wide-ranging adaptation potential – for example, *agriculture* – continue to receive only minimal finance. Mainstreaming adaptation and resilience into development pathways is imperative, particularly in highly vulnerable developing countries.

Moving forward, all actors must urgently work to scale the quantity and quality of climate finance. Key priorities for ensuring more and better climate finance include: *transforming the financial system* with an emphasis on concessional financing and de-risking; *bridging climate and development needs*, harnessing synergies to deliver co-benefits for both people and nature; *mobilizing domestic capital*, with an emphasis on enabling policies and regulatory frameworks; and *improving the availability and accessibility of quality, granular data* to measure and manage progress.
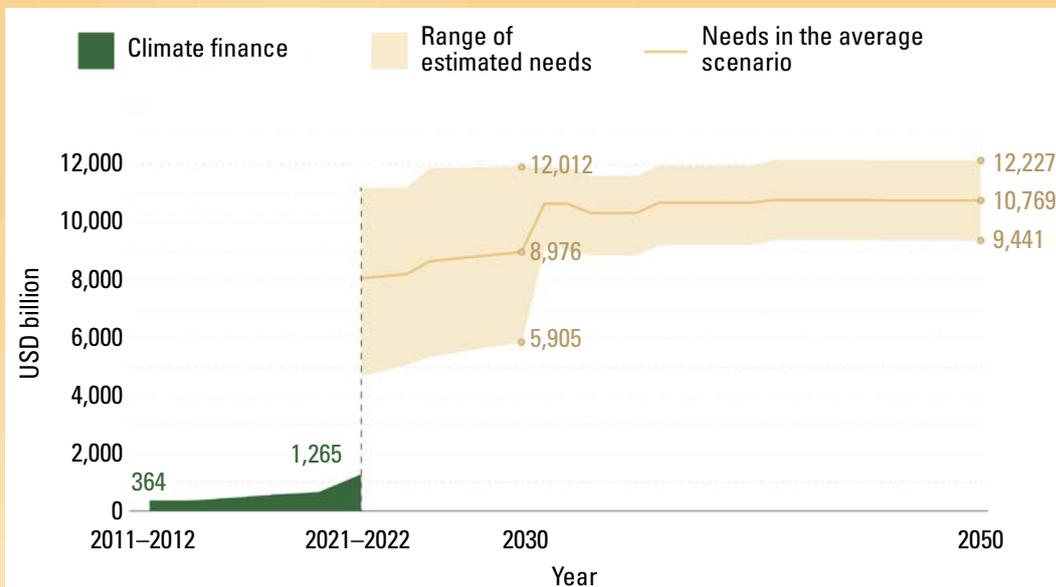
Figure 26. Global tracked climate finance and average estimated annual needs through 2050.

Source: Climate Policy Initiative

Data sets and methods

GREENHOUSE GASES DATA

Estimated concentrations from 1750 are used to represent pre-industrial conditions. Calculations assume a pre-industrial mole fraction of 278.3 ppm for CO_2, 729.2 ppb for CH_4 and 270.1 ppb for N_2O.

World Data Centre for Greenhouse Gases operated by Japan Meteorological Agency https://gaw.kishou.go.jp/.

World Meteorological Organization (WMO). *WMO Greenhouse Gas Bulletin – No. 19: The State of Greenhouse Gases in the Atmosphere Based on Global Observations through 2022*. Geneva, 2023.

GLOBAL TEMPERATURES DATA

GLOBAL MEAN TEMPERATURE SERIES

The method for calculating global mean temperature anomalies relative to an 1850–1900 baseline is based on the assessment of long-term change and its uncertainty made by Working Group I in its contribution to the IPCC Sixth Assessment Report (IPCC AR6 WG I). In 2021, the IPCC AR6 WG I assessed change from 1850–1900 to other periods based on an average of four data sets – HadCRUT5, Berkeley Earth, NOAA Interim and Kadow et al. (2020) – which start in 1850 and are globally or near-globally complete in the modern period.

To include shorter data sets, which can help to better understand recent temperature changes, in the present report, the estimate made by the IPCC for the temperature change between 1850–1900 and 1981–2010 is combined with estimated changes between 1981–2010 and the current year from six data sets to calculate anomalies for 2023 relative to 1850–1900. There is good agreement between the data sets on changes from 1981–2010 to the present, as this is a period with good observational coverage.

The additional uncertainty from the spread of the data sets is combined with that of the IPCC's estimate of the uncertainty in the change from 1850–1900 to 1981–2010. Global mean temperature anomalies were calculated relative to an 1850–1900 baseline using the following steps starting from time series of global monthly mean temperatures for each data set:

1. For each data set, anomalies were calculated relative to the 1981–2010 average by subtracting the mean for the period 1981–2010 for each month separately.

2. An annual mean anomaly was calculated from the monthly mean anomalies.

3. The amount of 0.69 °C was added to each series, based on the estimated difference between 1850–1900 and 1981–2010, calculated using the method from IPCC AR6 WG I (see caption for Figure 1.12 in that report).

4. The mean and standard deviation of the estimates were calculated.

5. The uncertainty in the IPCC estimate was combined with the standard deviation, assuming the two are independent and assuming the IPCC uncertainty range (0.54 °C to 0.79 °C) is representative of a 90% confidence range (1.645 standard deviations).

The number quoted in this report for 2023 (1.45 ± 0.12 °C) was calculated in this way with 1.45 °C being the mean of the seven estimates and 0.03 °C the standard deviation.

ANNUAL TEMPERATURE MAPS

For the map of temperature anomalies for 2023, a median of six data sets was used, regridded to the spatial grid of the lowest resolution data sets (NOAAGlobalTemp, and HadCRUT5), which are presented on a 5° latitude by 5° longitude grid. The median is used in preference to the mean to minimize the effect of potential outliers in individual grid cells. The half-range of the data sets provides an indication of the uncertainty. The spread between the data sets is largest at high latitudes and in Central Africa, both regions with sparse data coverage.

GLOBAL MEAN TEMPERATURE ANOMALIES FOR 2023 RELATIVE TO OTHER PERIODS

This table shows global mean temperature anomalies for individual data sets for 2023 relative to four different baselines. The uncertainty indicated for the three modern baselines (1981–2010, 1991–2020 and 1961–1990) are the standard deviations of the available estimates multiplied by 1.645 to represent the 90% uncertainty range.

Period	1850–1900	1981–2010	1991–2020	1961–1990
HadCRUT5	1.44	0.75	0.56	1.09
NOAA GlobalTemp	1.43	0.75	0.55	1.05
GISTEMP	1.44	0.75	0.56	1.07
Berkeley Earth	1.45	0.75	0.57	1.12
ERA5	1.48	0.79	0.60	1.12
JRA-55	1.43	0.74	0.56	1.09
Mean of six datasets	1.45±0.12	0.76±0.03	0.57±0.03	1.09±0.04

The following six data sets were used, including four traditional datasets:

HadCRUT.5.0.1.0: Morice, C. P.; Kennedy, J. J.; Rayner, N. A. et al. An Updated Assessment of Near-Surface Temperature Change From 1850: The HadCRUT5 Data Set. *Journal of Geophysical Research: Atmospheres* **2021**, *126*, e2019JD032361. https://doi.org/10.1029/2019JD032361. HadCRUT.5.0.2.0 data were obtained from http://www.metoffice.gov.uk/hadobs/hadcrut5 on 17 January 2024 and are © British Crown Copyright, Met Office 2024, provided under an Open Government Licence, http://www.nationalarchives.gov.uk/doc/open-government-licence/version/3/.

NOAA Interim: Vose, R. S.; Huang, B.; Yin, X. et al. Implementing Full Spatial Coverage in NOAA's Global Temperature Analysis. *Geophysical Research Letters* **2021**, *48*, e2020GL090873. https://doi.org/10.1029/2020GL090873.

GISTEMP v4: GISTEMP Team, 2022: *GISS Surface Temperature Analysis (GISTEMP), version 4*. NASA Goddard Institute for Space Studies, https://data.giss.nasa.gov/gistemp/. Lenssen, N.; Schmidt, G.; Hansen, J. et al. Improvements in the GISTEMP Uncertainty Model. *Journal of Geophysical Research: Atmospheres* **2019**, *124*, 6307–6326. https://doi.org/10.1029/2018JD029522.

Berkeley Earth: Rohde, R. A.; Hausfather, Z. The Berkeley Earth Land/Ocean Temperature Record. *Earth System Science Data* **2020**, *12*, 3469–3479. https://doi.org/10.5194/essd-12-3469-2020.

And two reanalyses:

JRA-55: Kobayashi, S.; Ota, Y.; Harada, Y. et al. The JRA-55 Reanalysis: General Specifications and Basic Characteristics. *Journal of the Meteorological Society of Japan*. Ser. II **2015**, *93*, 5–48. https://doi.org/10.2151/jmsj.2015-001.

ERA5: Hersbach, H.; Bell, B.; Berrisford, P. et al. *ERA5 Monthly Averaged Data on Single Levels from 1940 to Present*; Copernicus Climate Change Service (C3S) Climate Data Store (CDS), 2023. https://doi.org/10.24381/cds.f17050d7.

IPCC used an additional data set. Combining the six datasets used in this report with Kadow reduces the estimated global mean for 2023 by 0.01 C and increases the uncertainty range by a similar amount:

Kadow et al.: Kadow, C.; Hall, D. M.; Ulbrich, U. Artificial Intelligence Reconstructs Missing Climate Information. *Nature Geoscience* **2020** *13*, 408–413. https://doi.org/10.1038/s41561-020-0582-5.

A new reanalysis produced by JRA-3Q is now also available. JRA-55 was used in this report for consistency with the provisional statement released in December 2023. For comparison, the values for 2023 are shown relative to the four baselines for JRA-3Q and JRA-55 in the following table. Note that the replacement of JRA-55 with JRA-3Q in the mean of the six data sets has a negligible effect on the global mean temperature for 2023.

Period	1850–1900	1981–2010	1991–2020	1961–1990
JRA-3Q	1.47	0.78	0.58	1.11
JRA-55	1.43	0.74	0.56	1.07
Mean of six datasets using JRA-3Q	1.45±0.12	0.76±0.03	0.57±0.03	1.09±0.04

LAND TEMPERATURES AND SEA-SURFACE TEMPERATURES DATA

The land temperature assessment is based on three data sets:

CRUTEM.5.0.2.0: Osborn, T. J.; Jones, P. D.; Lister, D. H. et al. Land Surface Air Temperature Variations Across the Globe Updated to 2019: The CRUTEM5 Data Set. *Journal of Geophysical Research: Atmospheres* **2021**, *126 (2)*, e2019JD032352. https://doi.org/10.1029/2019JD032352.

CRUTEM.5.0.2.0 data were obtained from http://www.metoffice.gov.uk/hadobs/crutem5 on 17 January 2024 and are © British Crown Copyright, Met Office 2024, provided under an Open Government License, http://www.nationalarchives.gov.uk/doc/open-government-licence/version/3/.

GHCNv4: Menne, M. J.; Gleason, B. E.; Lawrimore, J. et al. Global Historical Climatology Network – Monthly Temperature [Global mean]. NOAA National Centers for Environmental Information, 1917. https://doi.org/10.7289/V5XW4GTH .

Berkeley Earth: Rohde, R. A.; Hausfather, Z. The Berkeley Earth Land/Ocean Temperature Record. *Earth System Science Data* **2020**, *12*, 3469–3479. https://doi.org/10.5194/essd-12-3469-2020.

The sea-surface temperature assessment is based on two data sets:

HadSST.4.0.1.0: Kennedy, J. J.; Rayner, N. A.; Atkinson, C. P. et al. An Ensemble Data Set of Sea
        Surface Temperature Change From 1850: The Met Office Hadley Centre HadSST.4.0.0.0
        Data Set. *Journal of Geophysical Research: Atmospheres* **2019**, *124 (14)*, 7719–7763. https://
        doi.org/10.1029/2018JD029867.
HadSST.4.0.1.0 data were obtained from http://www.metoffice.gov.uk/hadobs/hadsst4 on 17 January
        2024 and are © British Crown Copyright, Met Office 2024, provided under an Open
        Government License, http://www.nationalarchives.gov.uk/doc/open-government-licence/
        version/3/.
ERSSTv5: Huang B.; Thorne W. P.; Banzon V. F. et al. NOAA Extended Reconstructed Sea-Surface
        Temperature (ERSST), Version 5. [Global mean]. NOAA National Centers for Environmental
        Information. https://doi.org/10.7289/V5T72FNM.

OCEAN HEAT CONTENT DATA

The ensemble mean is an update of the outcome of a concerted international effort[123], and
all products used are referenced here. Note that global ocean heat content values are given
for the ocean surface area between 60°S-60°N and limited to areas deeper than 300 m in
each product. The value for 2022 is based on a subset of the products for which updates are
available. A baseline of 2005–2021 is used for the Ocean Heat Content time series (Figure 4)
as near-global coverage is available in this period thanks to the network of Argo sub-surface
floats.

The 2023 value is based on the estimate from Minière et al. (2023) and Cheng et al. (2017,
see below):

Minière, A.; von Schuckmann, K.; Sallée, J.-B. et al. Robust Acceleration of Earth System Heating
        Observed over the Past Six Decades. *Sci Rep* **2023**, *13 (1)*, 22975. https://doi.org/10.1038/
        s41598-023-49353-1.

DATA USED UP TO 2022:

Cheng, L.; Trenberth, K. E.; Fasullo, J. et al. Improved Estimates of Ocean Heat Content from 1960 to
        2015. *Science Advances* **2017**, *3*, e1601545. https://doi.org/10.1126/sciadv.1601545.
Gaillard, F.; Reynaud, T.; Thierry, V. et al. In Situ–Based Reanalysis of the Global Ocean Temperature
        and Salinity with ISAS: Variability of the Heat Content and Steric Height. *Journal of
        Climate* **2016**, *29*, 1305–1323. https://doi.org/10.1175/JCLI-D-15-0028.1.
Ishii, M.; Fukuda, Y.; Hirahara, S. et al. Accuracy of Global Upper Ocean Heat Content Estimation
        Expected from Present Observational Data Sets. *SOLA* **2017**, *13*, 163–167. https://doi.
        org/10.2151/sola.2017-030.
Kuusela, M.; Giglio, D. Global Ocean Heat Content Anomalies based on Argo Data (2.0.0). *Zenodo*
        2023. https://doi.org/10.5281/zenodo.7562281.
Levitus, S.; Antonov, J. I.; Boyer, T. P. et al. World Ocean Heat Content and Thermosteric Sea Level
        Change (0-2 000 m) 1955–2010. *Geophysical Research Letters* **2012**, *39*, L10603. https://
        doi.org/10.1029/2012GL051106.
Lyman, J. M.; Johnson, G. C. Estimating Global Ocean Heat Content Changes in the Upper 1800 m
        since 1950 and the Influence of Climatology Choice. *Journal of Climate* **2014**, *27*, 1945–
        1957. https://doi.org/10.1175/JCLI-D-12-00752.1.
von Schuckmann, K.; Le Traon, P.-Y. How Well Can We Derive Global Ocean Indicators from Argo
        Data? *Ocean Science* **2011**, *7*, 783–791. https://doi.org/10.5194/os-7-783-2011. Data
        available at: https://marine.copernicus.eu/access-data/ocean-monitoring-indicators.

ADDITIONAL DATA USED TO 2021:

Desbruyères, D. G.; Purkey, S. G.; McDonagh, E. L. et al. Deep and Abyssal Ocean Warming from 35 Years of Repeat Hydrography. *Geophysical Research Letters* **2016**, *43*, 310–356. https://doi.org/10.1002/2016GL070413.

Desbruyères, D.; McDonagh, E. L.; King, B. A. et al. Global and Full-Depth Ocean Temperature Trends during the Early Twenty-First Century from Argo and Repeat Hydrography. *Journal of Climate* **2017**, *30*, 1985–1997. https://doi.org/10.1175/JCLI-D-16-0396.1.

Good, S. A.; Martin, M. J.; Rayner, N. A. EN4: Quality Controlled Ocean Temperature and Salinity Profiles and Monthly Objective Analyses with Uncertainty Estimates. *Journal of Geophysical Research: Oceans* **2013**, *118*, 6704–6716. https://doi.org/10.1002/2013JC009067.

Hosoda, S.; Ohira, T.; Nakamura, T. A Monthly Mean Dataset of Global Oceanic Temperature and Salinity Derived from Argo Float Observations. *JAMSTEC Report of Research and Development* **2008**, *8*, 47–59. https://www.jstage.jst.go.jp/article/jamstecr/8/0/8_0_47/_article.

Kuusela M.; Stein, M. L. Locally Stationary Spatio-temporal Interpolation of Argo Profiling Float Data. *Proceedings of the Royal Society A* **2018**, *474*, 20180400. http://dx.doi.org/10.1098/rspa.2018.0400.

Li, H.; Xu, F.; Zhou, W. et al. Development of a Global Gridded Argo Data Set with Barnes Successive Corrections. *Journal of Geophysical Research: Oceans* **2017**, *122*, 866–889, https://doi.org/10.1002/2016JC012285.

Roemmich, D.; Gilson, J. The 2004–2008 Mean and Annual Cycle of Temperature, Salinity, and Steric Height in the Global Ocean from the Argo Program. *Progress in Oceanography* **2009**, *82*, 81–100. https://doi.org/10.1016/j.pocean.2009.03.004.

Roemmich, D.; Church, J.; Gilson, J. et al. Unabated Planetary Warming and its Ocean Structure Since 2006. *Nature Climate Change* **2015**, *5*, 240. https://doi.org/10.1038/nclimate2513.

IN ADDITION, DATA USED UP TO 2020:

Church, J. A.; White, N. J.; Konikow, L. F. et al. Revisiting the Earth's Sea-level and Energy Budgets from 1961 to 2008. *Geophysical Research Letters* **2011**, *38*. https://doi.org/10.1029/2011GL048794.

Domingues, C. M.; Church, J. A.; White, N. J. et al. Improved Estimates of Upper-ocean Warming and Multi-decadal Sea-level Rise. *Nature* **2008**, *453*, 1090–1093. https://doi.org/10.1038/nature07080.

Li, Y.; Church, J. A.; McDougall, T. J. et al. Sensitivity of Observationally Based Estimates of Ocean Heat Content and Thermal Expansion to Vertical Interpolation Schemes. *Geophysical Research Letters* **2022**, *49*, e2022G. https://doi.org/10.1029/2022GL101079.

Wijffels, S.; Roemmich, D.; Monselesan, D., et al. Ocean Temperatures Chronicle the Ongoing Warming of Earth. *Nature Climate Change* **2016**, 6, 116–118. https://doi.org/10.1038/nclimate2924.

SEA LEVEL DATA

GMSL from CNES/Aviso+ https://www.aviso.altimetry.fr/en/data/products/ocean-indicators-products/mean-sea-level/data-acces.html#c12195

Copernicus Climate Change Service (C3S), 2018: *Sea Level Daily Gridded Data from Satellite Observations for the Global Ocean from 1993 to Present*. C3S Climate Data Store (CDS), https://doi.org/10.24381/cds.4c328c78.

MARINE HEATWAVE AND MARINE COLD SPELL DATA

MHWs are categorized as moderate when the sea-surface temperature (SST) is above the ninetieth percentile of the climatological distribution for five days or longer; the subsequent categories are defined with respect to the difference between the SST and the climatological distribution average: strong, severe, or extreme, if that difference is, respectively, more than two, three or four times the difference between the ninetieth percentile and the climatological distribution average (Hobday et al., 2018). MCS categories are analogous but counting days below the tenth percentile, except for the "ice" category. This category is given to any MCS when the threshold for the occurrence on any given day of the event is below –1.7°C (Schlegel et la., 2021). These are therefore considered to be conditions related to sea-ice, and not extreme temperature fluctuations.

The baseline used for MHWs and MCSs is 1982–2011, which is shifted by one year from the standard normal period of 1981–2010 because the first full year of the satellite SST series on which it is based is 1982. This period has not been updated to the current standard normal period of 1991–2020 because the shifting of the baseline has a significant effect on the results and would not allow for comparison of MHW/MCS statistics with previous versions of this report.

All MHWs and MCSs are detected using the NOAA daily Optimum Interpolation Sea-Surface Temperature (OISST) v2.1 dataset (Huang et al. 2021).

Hobday, A. J.; Alexander, L. V.; Perkins, S. E. et al. A Hierarchical Approach to Defining Marine Heatwaves. *Progress in Oceanography* **2016**, *141*, 227–238. https://doi.org/10.1016/j.pocean.2015.12.014.

Hobday, A. J.; Oliver, E. C. J.; Sen Gupta, A. et al. Categorizing and Naming Marine Heatwaves. *Oceanography* **2018**, *31* (2), 1–13. https://www.jstor.org/stable/26542662.

Huang, B.; Liu, C.; Banzon, V. et al. Improvements of the Daily Optimum Interpolation Sea Surface Temperature (DOISST) Version 2.1. *Journal of Climate* **2021**, *34 (8)*, 2923–2939. https://doi.org/10.1175/JCLI-D-20-0166.1.

Schlegel, R. W.; Darmaraki, S.; Benthuysen, J. A. et al. Marine Cold-Spells. *Progress in Oceanography* **2021**, *198*, 102684. https://doi.org/10.1016/j.pocean.2021.102684.

ICE SHEETS DATA

Mankoff, K. D.; Fettweis, X.; Langen, P. L. et al. Greenland Ice Sheet Mass Balance from 1840 through Next Week. *Earth System Science Data* **2021**, *13* (10), 5001–5025. https://doi.org/10.5194/essd-13-5001-2021.

Gravimetric (GRACE) ice mass time series for the Greenland and Antarctic Ice Sheets are calculated using spherical harmonics from JPL RL06v1, following Velicogna et al (2020). The degree-1 geocentre terms are calculated using Sutterley and Velicogna (2019), using Loomis et al (2020) C2.0 and C3.0 coefficients. The GRACE/GRACE-FO data are corrected for the long-term trend of glacial isostatic adjustment (GIA) from the solid earth using the regional IJ05 R2 GIA model (Ivins et al., 2013) over Antarctica and the regional Simpson et al. (2009) GIA model over Greenland. These regional GIA models do not include realistic GIA signal outside the ice sheets. For this reason, outside of Greenland and Antarctica, GIA corrections are based on Geruou et al. (2013) with the ICE6G ice history (Peltier et al., 2015).

Geruo A.; Wahr, J.; Zhong, S. Computations of the Viscoelastic Response of a 3-D Compressible Earth to Surface Loading: An Application to Glacial Isostatic Adjustment in Antarctica and Canada. *Geophysical Journal International* **2013**, *192 (2)*, 557–572. https://doi.org/10.1093/gji/ggs030.

Ivins, E. R.; James, T. S.; Wahr, J. et al. Antarctic Contribution to Sea Level Rise Observed by GRACE with Improved GIA Correction. *Journal of Geophysical Research: Solid Earth* **2013**, *118*, 3126–3141. https://doi.org/10.1002/jgrb.50208.

Loomis, B. D.; Rachlin, K. E.; Luthcke, S. B. Improved Earth Oblateness Rate Reveals Increased Ice Sheet Losses and Mass-driven Sea Level Rise. *Geophysical Research Letters* **2019,** *46*, 6910–6917. https://doi.org/10.1029/2019GL082929.

Peltier, W. R.; Argus, D. F.; Drummond, R. Space Geodesy Constrains Ice Age Terminal Deglaciation: The Global ICE-6G_C (VM5a) Model. *Journal of Geophysical Research: Solid Earth* **2015**, *120 (1)*, 450–487. https://doi.org/10.1002/2014JB011176.

Simpson, M. J.; Milne, G. A.; Huybrechts, P. et al. Calibrating a Glaciological Model of the Greenland Ice Sheet from the Last Glacial Maximum to Present-day Using Field Observations of Relative Sea Level and Ice Extent. *Quaternary Science Reviews* **2009**, *28* (17), 1631–1657. https://doi.org/10.1016/j.quascirev.2009.03.004.

Sutterley, T. C.; Velicogna, I. Improved Estimates of Geocenter Variability from Time-variable Gravity and Ocean Model Outputs. *Remote Sensing* **2019**, *11* (18), 2108. https://doi.org/10.3390/rs11182108.

Velicogna I.; Mohajerani Y.; A, G. et al. Continuity of Ice Sheet Mass Loss in Greenland and Antarctica from the GRACE and GRACE Follow-On Missions, *Geophysical Research Letters* **2020,** *47*, e2020GL087291. https://doi.org/10.1029/2020GL087291.

GLACIERS DATA

Global glacier monitoring information is provided by the World Glacier Monitoring Service:

World Glacier Monitoring Service (WGMS). Fluctuations of Glaciers Database, World Glacier Monitoring Service (WGMS) 2024. Zurich, Switzerland. https://doi.org/10.5904/wgms-fog-2024-01.

SEA-ICE DATA

Data are from the EUMETSAT OSI SAF Sea-Ice Index v2.2 (OSI-SAF, based on Lavergne et al., 2019 – https://osisaf-hl.met.no/v2p2-sea-ice-index) and the National Snow and Ice Data Center (NSIDC) v3 Sea-Ice Index (Fetterer et al., 2017). Sea-ice concentrations are estimated from microwave radiances measured from satellites. Extent is the area of ocean grid cells where the sea-ice concentration exceeds 15%. There are modest differences in the absolute extent between data sets, but they agree well on the year-to-year changes and trends. In the main text of the report, NSIDC values are reported for absolute extents, and rankings. Comparison figures for OSI SAF are given in the table below.

Metric	NSIDC	OSI SAF
Arctic daily minimum	4.23 million km², 19 September Sixth lowest on record	4.71 million km2, 16 September Sixth lowest on record
Arctic daily minimum	4.62 million km², 6 March Fifth lowest on record	14.64 million km2, 3 March
Arctic daily minimum	1.79 million km², 21 February Lowest on record	2.0 million km2, 16 February Lowest on record
Arctic daily minimum	16.96 million km², 10 September Lowest on record	17.6 million km2, 12 September Lowest on record

OSI SAF Sea-ice index 1978-onwards, version 2.2 (2023), OSI-420. EUMETSAT Ocean and Sea-Ice Satellite Application Facility. Data extracted from Sea-ice index | OSI SAF (eumetsat.int).

Fetterer, F.; Knowles, K.; Meier, W. N. et al., 2017, updated daily. Sea Ice Index, Version 3. Boulder, Colorado, USA. National Snow and Ice Data Center (NSIDC), https://nsidc.org/data/G02135/versions/3.

Lavergne, T. Sørensen, A. M.; Kern, S. et al. Version 2 of the EUMETSAT OSI SAF and ESA CCI Sea-Ice Concentration Climate Data Records. *The Cryosphere* **2019**, *13* (1), 49–78. https://doi.org/10.5194/tc-13-49-2019.

PRECIPITATION DATA

The following Global Precipitation Climatology Centre (GPCC) data sets were used in the analysis:

- First Guess Monthly, https://doi.org/10.5676/DWD_GPCC/FG_M_100

- Monitoring Product (Version 2022), https://doi.org/10.5676/DWD_GPCC/MP_M_V2022_100

- Full Data Monthly (Version 2022), https://doi.org/10.5676/DWD_GPCC/FD_M_V2022_100

- Precipitation Climatology (Version 2022), https://doi.org/10.5676/DWD_GPCC/CLIM_M_V2022_100

In Figure 23, Iceland is shown as being much drier than the long-term average and parts of China much wetter. These features are due to a change in the way that real time data are processed and are not reflective of actual conditions.

List of contributors

WMO MEMBERS

Algeria, Andorra, Argentina, Armenia, Australia, Azerbaijan, Bahrain, Barbados, Belgium, Belize, Bosnia and Herzegovina, Brazil, Brunei, Bulgaria, Canada, Chile, China, Côte d'Ivoire, Croatia, Cyprus, Czech Republic, Denmark, Ecuador, Estonia, Finland, France, Georgia, Germany, Hungary, Iceland, India, Iran (Islamic Republic of), Ireland, Israel, Italy, Japan, Jordan, Kazakhstan, Latvia, Libya, Lithuania, Luxembourg, Malaysia, Mali, Mauritius, Mexico, Morocco, Myanmar, Netherlands, New Zealand, Nigeria, Norway, Pakistan, Panama, Paraguay, Peru, Poland, Republic of Korea, Republic of Moldova, Russian Federation, Saudi Arabia, Senegal, Serbia, Singapore, Slovakia, Slovenia, South Africa, Sweden, Switzerland, Thailand, Türkiye, Ukraine, United Arab Emirates, United Kingdom of Great Britain and Northern Ireland, United Republic of Tanzania, United States of America, Uruguay, Venezuela (Bolivarian Republic of), Viet Nam.

INDIVIDUAL CONTRIBUTORS

Vicente Anzellini (IDMC), Omar Baddour (WMO), Paul M Barker (University of New South Wales), Joseph Basconcillo (PAGASA), Hamid Bastani (WMO), Jorge Alvar-Beltrán (FAO), Jana Birner (UNHCR), Nicholas Bishop (IOM), Jessica Blunden (NOAA), Roberta Boscolo (WMO), Tim Boyer (NOAA NCEI), Anny Cazanave (Legos), Xuan Che (UNDRR), Lijing Cheng (Institute of Atmospheric Physics (IAP), Center for Ocean Mega-Science), John Church (University of New South Wales), Damien Desbruyeres (Ifremer), Catia Domingues (NOC), Robert Dunn (Met Office), Arianna Gialletti (FAO), Pini Giancarlo (WFP), Donata Giglio (University of Colorado), John E Gilson (SCRIPPS), Alashiya Gordes (FAO), Atsushi Goto (WMO), Sarah Grimes (WMO), Flora Gues (CELAD, Mercator Ocean International), Peer Hechler (WMO), Christopher Hewitt (WMO), Shigeki Hosoda (JAMSTEC), Matthias Huss (ETH Zürich), Amanda Ignatia (UNHCR), Kirsten Isensee (IOC/UNESCO), Piyush Jain (Northern Forestry Centre), Gregory C Johnson (NOAA PMEL), Christopher Kadow (DKRZ), Hideki Kanamaru (FAO), Maarten Kappelle (UNEP), John Kennedy (WMO Expert), Rachel Killick (Met Office), Brian King (NOC), Nicolas Kolodziejczyk (University of Brest), Animesh Kumar (UNDRR), Mikael Kuusela (Carnegie Mellon University), Gernot Laganda (WFP), Lancelot Leclercq (Legos), Yuehua Li (Yunnan University), Ricardo Locarnini (NOAA NCEI), John Lyman (NOAA PMEL), Shawn Marshall (Environment and Climate Change Canada (ECCC) and University of Calgary), Jesse Mason (WFP), Jutta May (UNDRR), Trevor McDougall (University of New South Wales), Brian Menounos (University of Northern British Columbia), Atsushi Minami (JMA), Audrey Minère (Mercator Ocean International), Oe Mitsuho (JMA), Didier Paolo Monselesan (CSIRO), Sarah Purkey (Scripps), James Reagan (NOAA NCEI, University of Maryland), Dean Roemmich (Scripps), Lev Neretin (FAO), Julien Nicolas (ECMWF), Elisabeth Du Parc (IOM), Sylvain Ponserre (IDMC), Ileana Sinziana Puscas (IOM), Claire Ransom (WMO), David Robinson (Rutgers State University of New Jersey), Bonifacio Rogerio (WFP), Yousuke Sawa (JMA), Kanako Sato (JAMSTEC), Abhishek Savita (GEOMAR), Robert W Schlegel (Sorbonne Université, CNRS, Laboratoire d'Océanographie de Villefranche), Katherina Schoo (IOC/UNESCO), Serhat Sensoy (Turkish State Meteorological Service), Fumi Sezaki (JMA), Jose Álvaro Silva (WMO), Mike Sparrow (WMO/WCRP), Johan Stander (WMO), Martin Stendel (DMI), Toshio Suga (Tohoku University, JAMSTEC), Oksana Tarasova (WMO), Caterina Tassone (WMO/GCOS), Blair Trewin (Bureau of Meteorology), Thea Turkington (Meteorological Services Singapore/ASEAN Specialized Meteorological Centre), Isabella Velicogna (University of California), Alex Vermeulen (ICOS), Karina von Schuckmann (Mercator Ocean International), Ying Wang (UNEP), Susan E. Wjiffels (CSIRO, Woods Hole), Abdel-Lathif Younous (WFP), Markus Ziese (DWD, GPCC).

INSTITUTIONS

Bureau of Meteorology, Australia; Carnegie Mellon University, USA; Center for Ocean Mega-Science, Chinese Academy of Sciences, China; CELAD, France; Commonwealth Scientific and Industrial Research Organization, CSIRO Oceans and Atmosphere, Tasmania, Australia; Deutsches Klimarechenzentrum, DKRZ, Germany; Deutscher Wetterdienst, DWD, Germany; European Centre for Medium-range Weather Forecasts, ECMWF, UK; Environment and Climate Change Canada, ECCC, Canada; ETH Zürich; GEOMAR Helmholtz Centre for Ocean Research Kiel, Germany; Global Precipitation Climatology Centre, GPCC, Germany; Hong Kong Observatory; Ifremer, France; Institute of Atmospheric Physics, IAP, Chinese Academy of Sciences, China; Internal Displacement Monitoring Centre (IDMC); Japan Agency for Marine Earth Science and Technology, JAMSTEC, Japan; Japan Meteorological Agency, JMA, Japan; Laboratoire d'Océanographie de Villefranche, France; Legos, France; Met Office, UK; Mercator Ocean International, France; National Oceanic and Atmospheric Administration (NOAA) National Centres for Environmental Information (NCEI), USA; National Oceanic and Atmospheric Administration (NOAA) Pacific Marine Environmental Laboratory (PMEL), USA; National Oceanography Centre, Southampton, UK ; Northern Forestry Centre, Canadian Forest Service, Natural Resources Canada, Canada; Ocean Scope, France ; Rutgers State University of New Jersey; Scripps Institution of Oceanography, University of California San Diego, USA; Sorbonne Université, France; Tohoku University, Japan ; Turkish State Meteorological Service, Türkiye; University of Brest, France ; University of Calgary, Canada; University of Colorado, USA; Cooperative Institute for Satellite Earth Systems Studies, University of Maryland, USA ; University of New South Wales, Australia; University of Northern British Columbia; Woods Hole Oceanographic Institution, USA; Yunnan University, China;

UN AGENCIES

Food and Agriculture Organization of the United Nations (FAO), Intergovernmental Oceanographic Commission – United Nations Educational, Scientific and Cultural Organization (IOC-UNESCO), International Organization for Migration (IOM), United Nations Environment Programme (UNEP), United Nations High Commissioner for Refugees (UNHCR), United Nations Office for Disaster Risk Reduction (UNDRR), World Food Programme (WFP)

Endnotes

1   Trewin, B.; Cazenave, A.; Howell, S. et al. Headline Indicators for Global Climate Monitoring, *Bulletin of the American Meteorological Society* **2021** *102* (1), E20–E37. https://doi.org/10.1175/BAMS-D-19-0196.1.

2   World Meteorological Organization (WMO). *Climate Indicators and Sustainable Development: Demonstrating the Interconnections* (WMO-No. 1271). Geneva, 2021.

3   World Meteorological Organization (WMO). *United in Science 2023*: Sustainable development edition; WMO: Geneva, 2023.

4   United Nations; Department of Economic and Social Affairs. *Synergy Solutions for a World in Crisis: Tackling Climate and SDG Action Together*; 2023. https://sdgs.un.org/synergy-solutions-world-crisis-tackling-climate-and-sdg-action-together.

5   Betts, R. A.; Jones, C. D.; Knight, J. R. et al. El Niño and a Record CO_2 Rise. *Nature Clim Change* **2016**, *6* (9), 806–810. https://doi.org/10.1038/nclimate3063.

6   National Oceanic and Atmospheric Administration (NOAA). *Trends in Atmospheric Carbon Dioxide*. https://gml.noaa.gov/ccgg/trends/mlo.html. Measurements at Mauna Loa were interrupted by a volcanic eruption and the measurement site was temporarily relocated to Maunakea observatories 21 miles to the north.

7   Commonwealth Scientific and Industrial Research Organisation (CSIRO). *Latest Kennaook / Cape Grim greenhouse gas data. The latest greenhouse gas (GHG) data updated monthly from one of the cleanest air sources in the world*. https://www.csiro.au/greenhouse-gases/.

8   For anomalies relative to other baselines see Global mean temperature anomalies for 2023 relative to other periods..

9   Rantanen, M.; Laaksonen, A. The Jump in Global Temperatures in September 2023 Is Extremely Unlikely Due to Internal Climate Variability Alone. *npj Clim Atmos Sci* **2024**, *7* (1), 1–4. https://doi.org/10.1038/s41612-024-00582-9.

10 Hansen, J.; Sato, M.; Kharecha, P. et al. Earth's Energy Imbalance and Implications. *Atmospheric Chemistry and Physics* **2011**, *11* (24), 13421–13449. https://doi.org/10.5194/acp-11-13421-2011.

11 von Schuckmann, K.; Palmer, M. D.; Trenberth, K. E. et al. An Imperative to Monitor Earth's Energy Imbalance. *Nature Clim Change* **2016**, *6* (2), 138–144. https://doi.org/10.1038/nclimate2876.

12 von Schuckmann et al. (2020). Heat stored in the Earth system: where does the energy go? Earth Syst. Sci. Data, 12(3), 2013–2041. https://doi.org/10.5194/essd-12–2013–2020

13 Cheng, L.; Trenberth, K. E.; Fasullo, J. et al. Improved Estimates of Ocean Heat Content from 1960 to 2015. *Science Advances* **2017**, *3* (3), e1601545. https://doi.org/10.1126/sciadv.1601545.

14 Intergovernmental Panel on Climate Change (IPCC), 2019: Summary for Policymakers. In: *IPCC Special Report on the Ocean and Cryosphere in a Changing Climate,* https://www.ipcc.ch/site/assets/uploads/sites/3/2022/03/01_SROCC_SPM_FINAL.pdf.

15 Cheng, L.; Abraham, J.; Trenberth, K. E. et al. New Record Ocean Temperatures and Related Climate Indicators in 2023. *Adv. Atmos. Sci.* **2024**. https://doi.org/10.1007/s00376-024-3378-5.

16 von Schuckmann, K.; Minière, A.; Gues, F. et al. Heat Stored in the Earth System 1960–2020: Where Does the Energy Go? *Earth System Science Data* **2023**, *15* (4), 1675–1709. https://doi.org/10.5194/essd-15-1675-2023. Loeb, N. G.; Johnson, G. C.; Thorsen, T. J. et al. Satellite and Ocean Data Reveal Marked Increase in Earth's Heating Rate. *Geophysical Research Letters* **2021**, *48* (13), e2021GL093047. https://doi.org/10.1029/2021GL093047.

17 Minière, A.; von Schuckmann, K.; Sallée, J.-B. et al. Robust Acceleration of Earth System Heating Observed over the Past Six Decades. *Sci Rep* **2023**, *13* (1), 22975. https://doi.org/10.1038/s41598-023-49353-1.

18 Minière, A.; von Schuckmann, K.; Sallée, J.-B. et al. Robust Acceleration of Earth System Heating Observed over the Past Six Decades. *Sci Rep* **2023**, *13* (1), 22975. https://doi.org/10.1038/s41598-023-49353-1.

19 Raghuraman, S. P.; Paynter, D.; Ramaswamy, V. Anthropogenic Forcing and Response Yield Observed Positive Trend in Earth's Energy Imbalance. *Nat Commun* **2021**, *12* (1), 4577. https://doi.org/10.1038/s41467-021-24544-4. Kramer, R. J.; He, H.; Soden, B. J. et al. Observational Evidence of Increasing Global Radiative Forcing. *Geophysical Research Letters* **2021**, *48* (7), e2020GL091585. https://doi.org/10.1029/2020GL091585.

20 e.g., Loeb, N. G.; Johnson, G. C.; Thorsen, T. J. et al. Satellite and Ocean Data Reveal Marked Increase in Earth's Heating Rate. *Geophysical Research Letters* **2021**, *48* (13), e2021GL093047. https://doi.org/10.1029/2021GL093047. Hakuba, M. Z.; Frederikse, T.; Landerer, F. W. Earth's Energy Imbalance From the Ocean Perspective (2005–2019). *Geophysical Research Letters* **2021**, *48* (16), e2021GL093624. https://doi.org/10.1029/2021GL093624.

21 Purkey, S. G.; Johnson, G. C. Warming of Global Abyssal and Deep Southern Ocean Waters between the 1990s and 2000s: Contributions to Global Heat and Sea Level Rise Budgets. *Journal of Climate* **2010**, *23* (23), 6336–6351. https://doi.org/10.1175/2010JCLI3682.1.

22 Cheng, L.; Abraham, J.; Trenberth, K. E. et al. Another Year of Record Heat for the Oceans. *Adv. Atmos. Sci.* **2023**, *40* (6), 963–974. https://doi.org/10.1007/s00376-023-2385-2. Cheng, L.; von Schuckmann, K.; Abraham, J. P. et al. Past and Future Ocean Warming. *Nat Rev Earth Environ* **2022**, *3* (11), 776–794. https://doi.org/10.1038/s43017-022-00345-1.

23 Changes of these percentages from the provisional report reflect an update to the Cheng et al. dataset, see Cheng, L.; Abraham, J.; Trenberth, K. E. et al. New Record Ocean Temperatures and Related Climate Indicators in 2023. *Adv. Atmos. Sci.* **2024**. https://doi.org/10.1007/s00376-024-3378-5.

24 Cheng, L.; von Schuckmann, K.; Abraham, J. P. et al. Past and Future Ocean Warming. *Nat Rev Earth Environ* **2022**, *3* (11), 776–794. https://doi.org/10.1038/s43017-022-00345-1.

25 Cheng, L.; Trenberth, K. E.; Fasullo, J. et al. Improved Estimates of Ocean Heat Content from 1960 to 2015. *Science Advances* **2017**, *3* (3), e1601545. https://doi.org/10.1126/sciadv.1601545.

26 Smale, D. A.; Wernberg, T.; Oliver, E. C. J. et al. Marine Heatwaves Threaten Global Biodiversity and the Provision of Ecosystem Services. *Nat. Clim. Chang.* **2019**, *9* (4), 306–312. https://doi.org/10.1038/s41558-019-0412-1.

27 World Meteorological Organization (WMO). *WMO Greenhouse Gas Bulletin – No. 18: The State of Greenhouse Gases in the Atmosphere Based on Global Observations through 2021.* Geneva, 2022.

28 Friedlingstein, P.; O'Sullivan, M.; Jones, M. W. et al. Global Carbon Budget 2020. E*arth System Science Data* **2020**, *12* (4), 3269–3340. https://doi.org/10.5194/essd-12-3269-2020.

29 Intergovernmental Panel on Climate Change (IPCC). *Climate Change 2023: Synthesis Report. Contribution of Working Groups I, II and III to the Sixth Assessment Report of the Intergovernmental Panel on Climate Change*; Core Writing Team, H. Lee and J. Romero, Eds.; IPCC: Geneva, Switzerland, 2023. https://doi.org/10.59327/IPCC/AR6–9789291691647.

30 Intergovernmental Panel on Climate Change (IPCC), 2021: Climate Change 2021: The Physical Science Basis, Chapter 2, section 2.3.3.5 Ocean pH, https://www.ipcc.ch/report/ar6/wg1/.

31 Numbers in main text are from National Snow and Ice Data Center (NSIDC). OSI SAF figures are provided in Data sets and methods. https://nsidc.org/arcticseaicenews/2023/03/arctic-sea-ice-maximum-at-fifth-lowest-on-satellite-record/, https://nsidc.org/arcticseaicenews/2023/04/polar-dawn-to-dusk/.

32 National Snow and Ice Data Center (NSIDC). *Arctic sea ice minimum at sixth lowest extent on record.* https://nsidc.org/arcticseaicenews/2023/09/arctic-sea-ice-minimum-at-sixth/.

33 Fast December expansion, Arctic Sea Ice News and Analysis (nsidc.org) https://nsidc.org/arcticseaicenews/2024/01/fast-december-expansion/

34 1981–2010 is the period used by NSIDC for their monitoring

35 Liu, J.; Zhu, Z.; Chen, D. Lowest Antarctic Sea Ice Record Broken for the Second Year in a Row. *Ocean-Land-Atmosphere Research* **2023**, *2*, 0007. https://doi.org/10.34133/olar.0007.

36 Purich, A.; Doddridge, E. W. Record Low Antarctic Sea Ice Coverage Indicates a New Sea Ice State. *Commun Earth Environ* **2023**, *4* (1), 1–9. https://doi.org/10.1038/s43247-023-00961-9.

37 https://nsidc.org/arcticseaicenews/2023/09/antarctic-sets-a-record-low-maximum-by-wide-margin/.

38 Fast December expansion, Arctic Sea Ice News and Analysis (nsidc.org) https://nsidc.org/arcticseaicenews/2024/01/fast-december-expansion/.

39 The period 1981–2010 is used by NSIDC for their monitoring.

40 https://www.ipcc.ch/srocc/chapter/glossary/. Note that the Antarctic ice sheet can be further subdivided into West Antarctic, East Antarctic and the Antarctic Peninsula, but is treated here as a single entity.

41 Mankoff, K. D.; Fettweis, X.; Langen, P. L. et al. Greenland Ice Sheet Mass Balance from 1840 through next Week. *Earth System Science Data* **2021**, *13* (10), 5001–5025. https://doi.org/10.5194/essd-13-5001-2021.

42 National Snow and Ice Data Center (NSIDC). *Late-season melt spike*. https://nsidc.org/ice-sheets-today/analyses/late-season-melt-spike. *Sudden shift to southern heat*. https://nsidc.org/ice-sheets-today/analyses/sudden-shift-southern-heat.

43 Cumulative melt-day area is the area of the ice sheet that experienced melting conditions each day (diagnosed by the presence of liquid water at the surface), summed over the number of days in the melt season.

44 https://www.dmi.dk/nyheder/2023/varmerekorder-pa-indlandsisen/

45 Nghiem, S. V.; Hall, D. K.; Mote, T. L. et al. The Extreme Melt across the Greenland Ice Sheet in 2012. *Geophysical Research Letters* **2012**, *39* (20). https://doi.org/10.1029/2012GL053611.

46 Otosaka, I. N.; Shepherd, A.; Ivins, E. R. et al. Mass Balance of the Greenland and Antarctic Ice Sheets from 1992 to 2020. *Earth System Science Data* **2023**, *15* (4), 1597–1616. https://doi.org/10.5194/essd-15-1597-2023.

47 m w.e. is the depth of water equivalent to the change in ice thickness. Glacier ice is less dense than water, so the equivalent depth of water is slightly less than the thickness of ice lost.

48 WGMS (2023): Global Glacier Change Bulletin No. 5 (2020-2021). Michael Zemp, Isabelle Gärtner-Roer, Samuel U. Nussbaumer, Ethan Z. Welty, Inès Dussaillant, and Jacqueline Bannwart (eds.), ISC (WDS) / IUGG (IACS) / UNEP / UNESCO / WMO, World Glacier Monitoring Service, Zurich, Switzerland, 134 pp. Based on database version https://doi.org/10.5904/wgms-fog-2023-09.

49 Firn is multi-year snow, which has a higher albedo than glacier ice.

50 LiDAR stands for Light Detection and Ranging, which uses a laser to determine the height of the glacier surface.

51 Hugonnet, R.; McNabb, R.; Berthier, E. et al. Accelerated Global Glacier Mass Loss in the Early Twenty-First Century. *Nature* **2021**, *592* (7856), 726–731. https://doi.org/10.1038/s41586-021-03436-z.

52 Parisien, M.-A.; Barber, Q. E.; Flannigan, M. D. et al. Broadleaf Tree Phenology and Springtime Wildfire Occurrence in Boreal Canada. *Global Change Biology* **2023**, *29* (21), 6106–6119. https://doi.org/10.1111/gcb.16820.

53 Robinson, David A.; Estilow, Thomas W.; and NOAA CDR Program (2012): NOAA Climate Data Record (CDR) of Northern Hemisphere (NH) Snow Cover Extent (SCE), Version 1. NOAA National Centers for Environmental Information. https://doi.org/10.7289/V5N014G9.

54 IEA (2024), Renewables 2023, IEA, Paris https://www.iea.org/reports/renewables-2023

55 https://www.cop28.com/en/global-renewables-and-energy-efficiency-pledge

56 In general, a capacity factor is a measure of how often a power plant operates at its maximum capacity over a certain period, expressed as a percentage.

57 World Meteorological Organization (WMO), International Renewable Energy Agency (IRENA). 2022 Year in Review: Climate-driven Global Renewable Energy Potential Resources and Energy Demand. Geneva, 2023.

58 World Meteorological Organization (WMO). *WMO Greenhouse Gas Bulletin – No. 19: The State of Greenhouse Gases in the Atmosphere Based on Global Observations through 2022.* Geneva, 2022.

59 A Dobson unit is the depth (in units of 10 μm) of the pure gas you would get if it were extracted from the air column and reduced to standard temperature and pressure. 300 DU corresponds to 3mm.

60 https://ozonewatch.gsfc.nasa.gov/

61 https://atmosphere.copernicus.eu/monitoring-ozone-layer

62 https://mausam.imd.gov.in/responsive/monsooninformation.php

63 United Nations Environment Programme (UNEP). *Frontiers 2022: Noise, Blazes and Mismatches-Emerging Issues of Environmental Concern*. Nairobi, 2022.

64 Fire weather is weather conducive to wildfires, including high temperatures, low humidity, and high winds.

65 United Nations (UN). The Sustainable Development Goals Report 2022.; New York, 2022. https://unstats.un.org/sdgs/report/2022/.

66 United Nations (UN). The Sustainable Development Goals Report 2023: Special Edition. Towards a Rescue Plan for People and Planet; New York, 2023. https://unstats.un.org/sdgs/report/2023/.

67 https://www.mapa.gob.es/es/prensa/ultimas-noticias/el-146--del-territorio-est%C3%A1-en-emergencia-por-escasez-de-agua-y-el-274--en-alerta/tcm:30–659894

68 https://www.unocha.org/publications/report/libya/libya-flood-response-humanitarian-update-15-december-2023

69 https://reliefweb.int/report/greece/greece-severe-weather-and-floods-update-greek-civil-protection-hellenic-national-meteorological-service-copernicus-emsr-echo-daily-flash-11-september-2023

70 https://www.preventionweb.net/media/87994/download?startDownload=true

71 https://reliefweb.int/report/mozambique/unhcr-mozambique-cyclone-freddy-flash-update-3-24-march-2023

72 Internal Displacement Monitoring Centre (IDMC). 2023 Mid-year update. https://story.internal-displacement.org/2023-mid-year-update/.

73 https://sentinel-asia.org/EO/2023/article20230514MM.html

74 https://reliefweb.int/report/bangladesh/bangladesh-cyclone-mocha-humanitarian-response-situation-report-14-may-2023

75 National contribution

76 https://ahacentre.org/wp-content/uploads/2023/05/AHA-DRAFT-Situation_Report-9-TC-MOCHA-Myanmar-1.pdf

77 Internal Displacement Monitoring Centre (IDMC). 2023 Mid-year update. https://story.internal-displacement.org/2023-mid-year-update/.

78 United Nations High Commissioner for Refugees (UNHCR). Myanmar Emergency - Flash Update #2 on Cyclone Mocha. May 2023. https://data.unhcr.org/en/documents/details/100982.

79 https://www.nhc.noaa.gov/data/tcr/EP182023_Otis.pdf

80 EM-DAT. See also https://www.fitchratings.com/research/insurance/mexico-re-insurers-not-materially-affected-by-hurricane-otis-31-10-2023

81 https://reliefweb.int/report/mexico/mexico-hurricane-otis-situation-report-no-01-8-november-2023

82 https://www.treasury.govt.nz/sites/default/files/2023–04/impacts-from-the-north-island-weather-events.pdf

83 Merlone, A.; Pasotti, L.; Musacchio, C. et al. Evaluation of the Highest Temperature WMO Region VI Europe (Continental): 48.8°C, Siracusa Sicilia, Italy on August 11, 2021. *International Journal of Climatology* **2024**, *44* (3), 721–728. https://doi.org/10.1002/joc.8361.

84 https://meteofrance.com/actualites-et-dossiers/actualites/fortes-chaleurs-aout-2023

85 https://atmosphere.copernicus.eu/2023-year-intense-global-wildfire-activity

86 Government of Canada. *Canada's top 10 weather stories of 2023*. https://www.canada.ca/en/environment-climate-change/services/top-ten-weather-stories/2023.html

87 Jain, P.; Barber, Q. E.; Taylor, S. et al. Canada Under Fire – Drivers and Impacts of the Record-Breaking 2023 Wildfire Season; preprint; *ESS Open Archive*. February 28, **2024**. https://doi.org/10.22541/essoar.170914412.27504349/v1.

88 https://www.disastercenter.com/FEMA%20Daily%20Ops%20Briefing%20085–2023.pdf

89 NOAA Billion-dollar disasters https://www.ncei.noaa.gov/access/billions/events/US/2023?disasters[]=wildfire

90 Federal Emergency Management Agency (FEMA). Preliminary Damage Assessment Report https://www.fema.gov/sites/default/files/documents/PDAReport_FEMA4724DRexpedited-HI.pdf

91 Porto de Manaus - Estação Hidroviária do Amazonas. *Nível do Rio Negro > Níveis Máximo e Mínimo*. https://www.portodemanaus.com.br/?pagina=niveis-maximo-minimo-do-rio-negro

92 Ethiopia: Oct-Nov-Dec rainy season - Flash Update 1 - As of 18 December 2023 https://www.unocha.org/publications/report/ethiopia/ethiopia-oct-nov-dec-rainy-season-flash-update-1-18-december-2023. Kenya: Heavy Rains and Floods

Impact and Response (as of 20 December 2023) https://www.unocha.org/publications/report/kenya/kenya-heavy-rains-and-floods-impact-and-response-20-december-2023. Somalia Situation Report, 26 Dec 2023 https://www.unocha.org/publications/report/somalia/somalia-situation-report-26-dec-2023.

93 International Organization for Migration (IOM), *DTM East and Horn of Africa: Flood Snapshot (July - November 2023)*. IOM, East and the Horn of Africa. Dec 22 2023. https://dtm.iom.int/reports/east-and-horn-africa-flood-snapshot-july-november-2023

94 Horn of Africa Drought: Human Mobility Snapshot (January - June 2023) https://dtm.iom.int/reports/horn-africa-drought-human-mobility-snapshot-january-june-2023, https://dtm.iom.int/reports/horn-africa-drought-human-mobility-snapshot-january-june-2023?close=true

95 National contribution.

96 https://www.fao.org/3/cc6806en/cc6806en.pdf

97 United Nations (UN). The Sustainable Development Goals Report 2022.; New York, 2022. https://unstats.un.org/sdgs/report/2022/.

98 United Nations (UN). The Sustainable Development Goals Report 2023: Special Edition. Towards a Rescue Plan for People and Planet; New York, 2023. https://unstats.un.org/sdgs/report/2023/.

99 WFP. November 2023. WFP Global Operational Response Plan 2023. Update #9. Available at: https://docs.wfp.org/api/documents/WFP-0000153758/download/?_ga=2.87190362.312982961.1705667005-702211395.1695286933

100 Food and Agriculture Organization (FAO), IFAD, UNICEF, WFP and WHO. 2023. The State of Food Security and Nutrition in the World 2023. Urbanization, agrifood systems transformation and healthy diets across the rural–urban continuum. Rome, FAO. https://doi.org/10.4060/cc3017en

101 WFP. June 2023. WFP Global Operational Response Plan 2023. Update #8. Available at: docs.wfp.org/api/documents/WFP-0000150404/download/

102 Food and Agriculture Organization (FAO). 2023. Crop Prospects and Food Situation – Quarterly Global Report No. 2, July 2023. Rome. https://doi.org/10.4060/cc6806en

103 Food and Agriculture Organization (FAO), IFAD, UNICEF, WFP and WHO. 2023. The State of Food Security and Nutrition in the World 2023. Urbanization, agrifood systems transformation and healthy diets across the rural–urban continuum. Rome, FAO. https://doi.org/10.4060/cc3017en

104 Food and Agriculture Organization (FAO). 2021. The impact of disasters and crises on agriculture and food security: 2021. Rome. https://doi.org/10.4060/cb3673en

105 Food and Agriculture Organization (FAO). 2023. The Impact of Disasters on Agriculture and Food Security 2023 – Avoiding and reducing losses through investment in resilience. Rome. https://doi.org/10.4060/cc7900en

106 Food and Agriculture Organization (FAO). 2023. Crop Prospects and Food Situation – Triannual Global Report No. 3, November 2023. Rome. https://doi.org/10.4060/cc8566en

107 Food and Agriculture Organization (FAO). 2023. Crop Prospects and Food Situation – Triannual Global Report No. 3, November 2023. Rome. https://doi.org/10.4060/cc8566en

108 WFP. 2023. Indonesia - Monitoring Bulletin: July-September (Q3) 2023. https://www.wfp.org/publications/indonesia-monitoring-bulletin-july-september-q3-2023

109 OCHA. 2023. Latin America & The Caribbean Weekly Situation Update (As of 4 September 2023). https://reliefweb.int/report/cuba/latin-america-caribbean-weekly-situation-update-4-september-2023

110 Food and Agriculture Organization (FAO). 2023. Crop Prospects and Food Situation – Triannual Global Report No. 3, November 2023. Rome. https://doi.org/10.4060/cc8566en

111 Food and Agriculture Organization (FAO). 2023. Storm Daniel, Libya, September 2023. Rapid impact assessment of the flood on agriculture and livelihoods. DIEM-Impact assessment, FAO. September 13, 2023 https://data-in-emergencies.fao.org/apps/e451e32a054847469b1c1c731a8e5cff/explore

112 UN Refugee Agency warns of extreme hardship for forcibly displaced families this winter | UNHCR

[113] https://go.ifrc.org/emergencies/6435, https://reliefweb.int/disaster/fl-2023-000068-yem

[114] https://dtm.iom.int/reports/migration-along-eastern-corridor-july-2023

[115] https://reliefweb.int/report/pakistan/early-needs-identification-report-monsoon-flood-affected-areas-pakistan-august-2023

[116] Displacements Monitored by UNHCR Protection and Return Monitoring Network (PRMN)

[117] UNHCR Somalia Factsheet: December 2023 https://reliefweb.int/report/somalia/unhcr-somalia-factsheet-december-2023

[118] https://reliefweb.int/report/libya/libya-impact-storm-daniel-update-displacement-and-needs-november-2023

[119] https://missingmigrants.iom.int/

[120] UNHCR Gender, Displacement, and Climate Change. July 2020. https://www.unhcr.org/protection/environment/5f21565b4/gender-displacement-and-climate-change.html

[121] United Nations Environment Programme (2022b). Climate Change and Security Partnership Project Final Report: March 2017-Feburary 2022. Nairobi. https://wedocs.unep.org/handle/20.500.11822/40549

[122] https://sendaiframework-mtr.undrr.org/publication/report-midterm-review-implementation-sendai-framework-disaster-risk-reduction-2015−2030

[123] von Schuckmann, K.; Cheng, L.; Palmer, M. D. et al. Heat Stored in the Earth System: Where Does the Energy Go? *Earth System Science Data* **2020**, *12* (3), 2013−2041. https://doi.org/10.5194/essd-12-2013-2020.

FAO Food and Agriculture Organization of the United Nations

UNHCR The UN Refugee Agency

IOM UN MIGRATION

WFP World Food Programme

For more information, please contact:

World Meteorological Organization

7 bis, avenue de la Paix – P.O. Box 2300 – CH 1211 Geneva 2 – Switzerland

Strategic Communications Office
Cabinet Office of the Secretary-General

Tel: +41 (0) 22 730 83 14 – Fax: +41 (0) 22 730 80 27

Email: communications@wmo.int

wmo.int

JN 24245